ARL-TR-93-11

Copy No. 10

Nonlinear Acoustics: Periodic Waveguide, Scattering of Sound by Sound, Three-Layer Fluid, Finite Amplitude Sound in a Medium Having a Distribution of Relaxation Processes, and Production of an Isolated Negative Pulse in Water

Fourth Annual Summary Report under Grant N00014-89-J-1109

David T. Blackstock

Applied Research Laboratories
The University of Texas at Austin
P. O. Box 8029 Austin, TX 78713-8029

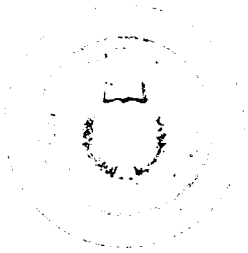

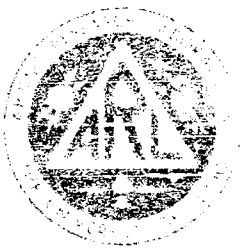

3 June 1993

Annual Report

1 October 1991 - 30 September 1992

Approved for public release:
Distribution unlimited.

Prepared for:
Office of Naval Research
Physics Division - Code 3120
800 North Quincy Street
Arlington, VA 22217-5660

REPORT DOCUMENTATION PAGE

Form Approved
OMB No. 0704-0188

1. AGENCY USE ONLY (Leave blank)	2. REPORT DATE	3. REPORT TYPE AND DATES COVERED
	3 June 1993	annual summary report, 1 Oct 91 - 30 Sep 92

4. TITLE AND SUBTITLE

Nonlinear Acoustics: Periodic Waveguide, Scattering of Sound by Sound, Three-Layer Fluid, Finite-Amplitude Sound in a Medium Having a Distribution of Relaxation Processes, and Production of an Isolated Negative Pulse in Water, Fourth Annual Summary Report under Grant N00014-89-J-1109

5. FUNDING NUMBERS

N00014-89-J-1109

6. AUTHOR(S)

Blackstock, David T.

7. PERFORMING ORGANIZATION NAMES(S) AND ADDRESS(ES)

Applied Research Laboratories
The University of Texas at Austin
P.O. Box 8029
Austin, Texas 78713-8029

8. PERFORMING ORGANIZATION REPORT NUMBER

ARL-TR-93-11

9. SPONSORING/MONITORING AGENCY NAME(S) AND ADDRESS(ES)

Office of Naval Research
Physics Division - Code 3120
800 North Quincy Street
Arlington, VA 22217-5660

10. SPONSORING/MONITORING AGENCY REPORT NUMBER

11. SUPPLEMENTARY NOTES

12a. DISTRIBUTION/AVAILABILITY STATEMENT

Approved for public release:
Distribution unlimited.

12b. DISTRIBUTION CODE

13. ABSTRACT (Maximum 200 words)

Research on nonlinear acoustics has been carried out during the 12-month period ending 30 September 1992. Progress is reported on the following projects.

(1) Propagation in a periodic waveguide
(2) Scattering of sound by sound
(3) Finite-amplitude waves in a three-layer fluid
(4) Finite-amplitude waves in a medium having a distribution of relaxation processes
(5) Propagation of an isolated negative-pressure pulse in water

14. SUBJECT TERMS

nonlinear acoustics, Bloch waves, periodic waveguide, dispersion, scattering of sound by sound, reflection, relaxing media, generalized Burgers equation, unipolar negative pulse

15. NUMBER OF PAGES

53

16. PRICE CODE

17. SECURITY CLASSIFICATION OF REPORT	18. SECURITY CLASSIFICATION OF THIS PAGE	19. SECURITY CLASSIFICATION OF ABSTRACT	20. LIMITATION OF ABSTRACT
UNCLASSIFIED	UNCLASSIFIED	UNCLASSIFIED	

TABLE OF CONTENTS

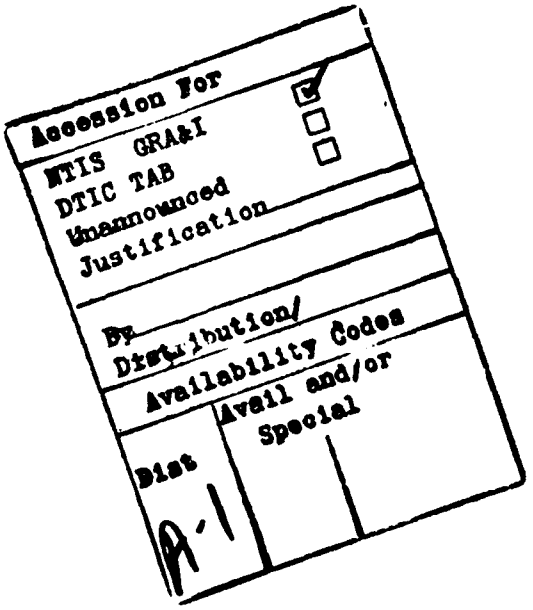

LIST OF FIGURES

1. INTRODUCTION

The research carried out under Grant N00014-89-J-1109, which began 1 October 1988 and is the successor to Contract N00014-84-K-0574, is primarily in the field of nonlinear acoustics. The broad goal is to determine the laws of behavior of finite-amplitude sound waves, especially to find generalizations of the known laws of linear acoustics. This report is the fourth annual report under the Grant and covers the 12-month period ending 30 September 1992. The previous report (third annual report[1]) is referred to herein as 91-5.*

The following persons participated in the research:

Graduate students

M. R. Bailey, M.S. student in Mechanical Engineering

C. E. Bradley, Ph.D. student in Mechanical Engineering

P. Li, Ph.D. student in Physics

J. A. Ten Cate, Ph.D. student in Mechanical Engineering; degree awarded May 1992

Y. Yazdi, M.S. student in Electrical and Computer Engineering

Three of these students received only partial support from the Grant. Bradley won a University Fellowship for the nine-month period beginning 1 September 1991. Ten Cate was partially supported by ONR Grant N00014-89-J-1003 (for which M. F. Hamilton is principal investigator) and the IR&D program of ARL:UT. Finally, beginning 1 January 1992, Yazdi's support came from the IR&D program of ARL:UT.

Senior personnel

M. F. Hamilton,† Mechanical Engineering Department, The University of Texas at Austin

*Numbers given in this style refer to items in the Chronological Bibliography given at the end of this report, e.g., 91-5 means the fifth entry in the list for 1991.

†Hamilton received no direct support from the Grant. However, he was co-supervisor of Ten Cate's Ph.D. research, which is described in Sec. 2.1 below.

W. M. Wright, Consultant, Physics Department, Kalamazoo College, Michigan

D. T. Blackstock, Principal Investigator

2. PROJECTS

The following projects were active during the report period:

- Propagation in a Periodic Waveguide
- Scattering of Sound by Sound
- Finite-Amplitude Waves in a 3-Layer Fluid
- Properties of Sea Water and Fresh Water for Finite-Amplitude Wave Calculations
- Finite-Amplitude Propagation in a Medium Having a Distribution of Relaxation Processes
- Production of an Isolated Negative Pressure Pulse in Water
- Miscellaneous

2.1 Propagation in a Periodic Waveguide

Bradley's project is a theoretical and experimental investigation of linear and nonlinear acoustic Bloch wave propagation in a periodic waveguide. The waveguide under study is a rigid, air-filled, rectangular duct loaded at regular intervals with rigidly terminated rectangular side branches. Previously reported on Bradley's project (89-6, 90-4, 91-5) were results of studies of linear and nonlinear time harmonic Bloch wave propagation and linear narrowband Bloch wave pulse propagation. This year four new topics were explored:

1. The propagation of the linear time harmonic Bloch waves that occur in an anisotropic periodic waveguide (i.e., a waveguide loaded with asymmetric scatterers).
2. The asymptotic behavior of linear Bloch wave pulses.
3. The propagation of nonlinear Bloch wave pulses.
4. The near-infinite group velocity of stop band Bloch wave pulses.

2.1.1 Anisotropic Periodic Waveguide

Because the side branches in all previously reported work have been symmetric (invariant under axial reversal), the periodic waveguide has been isotropic. To consider what sorts of Bloch wave solutions are possible in an anisotropic periodic waveguide, Bradley reduced the theory of Bloch waves in periodic waveguides to a very fundamental statement. The problem reduces to that of the eigenvalue problem associated with the unit cell translation operator

$$\mathbf{T}^C|\sigma\rangle = e^{jqh}|\sigma\rangle,$$

where $\mathbf{T}^C$ is the transmission matrix associated with the scatterer, $|\sigma\rangle$ is a column vector composed of the amplitudes of the conventional waves of which the Bloch wave is composed, q is the Bloch wave number, and h is the period of the waveguide. The eigenvalues yield the Bloch wave numbers (the Bloch dispersion relation) and the eigenvectors determine the conventional wave structure of the Bloch waves. For a very general class of scatterers, which include boundary deformations (as in the case of the side branches) and inclusions, the scattering is found to be reciprocal, even in the presence of thermoviscous acoustic boundary layer losses. It is found that, in terms of the Bloch wave number q, which accounts for the cell-to-cell structure, or *macrostructure* of the Bloch wave functions, the forward and backward traveling Bloch waves have the same form: $q^{(+)} = -q^{(-)}$ (the $(\pm)$ superscript denotes the forward and backward traveling Bloch waves). The analysis shows that this result is a direct consequence of the reciprocity of the scatterers. In other words, *reciprocity disallows birefringence.* In terms of the Bloch wave parameter g/f, which is derived from $|\sigma\rangle$ and accounts for the Bloch wave structure within a cell (i.e., the *microstructure*), the Bloch waves are *asymmetric*: $g/f^{(+)} \neq g/f^{(-)}$. Such asymmetry in the wave functions causes the Bloch acoustic impedance to be asymmetric as well: $Z_{Ba}^{(+)} \neq Z_{Ba}^{(-)}$. It is also found that the asymmetry resides primarily in the *phase* of g/f (in the lossless case $|g/f^{(+)}| = |g/f^{(-)}|$).

Measurements of $q^{(\pm)}$ and $g/f^{(\pm)}$ were made in the anisotropic periodic waveguide shown in Fig. 2.1(b). The waveguide used in past measurements (89-6, 90-6, 91-5), shown in Fig. 2.1(a), was made anisotropic by filling every third side branch and half filling the side branches on one side of the filled side branches. The asymmetric pair of side branches can be considered to be a single, asymmetric scatterer. The theoretical and experimental values of $\mathrm{Im}\{q^{(\pm)}\}$ and $\mathrm{Re}\{g/f^{(\pm)}\}$ are shown in Fig. 2.2. While there is some disparity between theory and experiment for $\mathrm{Im}\{q^{(\pm)}\}$, it is clear that $q^{(+)} = -q^{(-)}$ and $g/f^{(+)} \neq g/f^{(-)}$, in agreement with theoretical prediction.

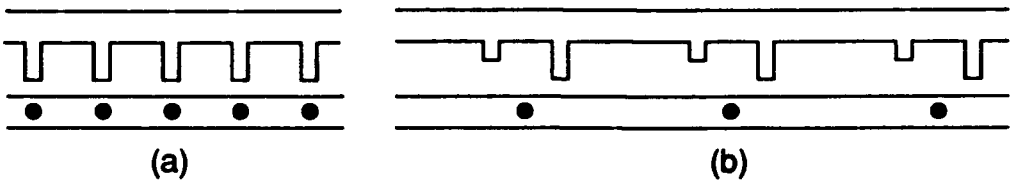

FIGURE 2.1
The (a) isotropic and (b) the anisotropic periodic waveguides.

AS-93-252

2.1.2 Asymptotic Behavior of Linear Bloch Wave Pulses

Asymptotic solutions of the problem of narrowband Bloch wave pulse propagation can be found by a stationary phase integration technique and use of the theory of asymptotic evaluation of Fourier integrals. The signal is introduced into the periodic medium via the boundary condition $p(z,t)|_{z=0} = A(t)e^{-j\omega_0 t}$. Here $A(t)$ is a narrowband envelope function with spectrum $F_{\text{env}}(\omega) = \int A(t)e^{j\omega t}dt$. Asymptotic solutions were found for three cases. In each case the frequency spectrum of the pulse includes a frequency associated with a different feature of the dispersion, as shown in Fig. 2.3. The three cases are:

I. The pulse spectrum is confined to a portion of the dispersion curve having nearly constant curvature. The asymptotic (large values of z) solution is

$$p(z,t) \sim \frac{C}{\sqrt{z}} F_{\text{env}}\left[-(t - z/c_{\text{gr}})/(q_0'' z)\right] e^{j[q_0 z - \omega_0 t + (t - z/c_{\text{gr}})^2/(2q_0'' z)]}, \qquad (2.1)$$

where $q_0 = q(\omega_0)$, $q_0'' = d^2q/d\omega^2(\omega_0)$, $c_{\text{gr}} = 1/\text{Re}\{q_0'\}$, and C is a constant. The pulse envelope distorts into its Fourier transform. Note that (1) the transformed envelope propagates at the group velocity, decays as $1/\sqrt{z}$, and spreads according to the factor $1/(q_0'' z)$, and (2) the carrier undergoes dispersive chirping, as shown by the $(t - z/c_{\text{gr}})^2$ term.

II. The pulse spectrum includes an inflection point frequency ω_i. The inflection frequency, defined by $\text{Re}\{q''(\omega_i)\} = 0$, has the largest group velocity in the spectral region. At the inflection, the stationary phase frequency undergoes a bifurcation, which makes it necessary to consider complex stationary phase frequencies. Concentrating on the leading edge of the pulse only, we find that the asymptotic (large values of z) solution is

$$p(z,t) \sim C F_{\text{env}}(\omega_i) \frac{1}{z^{1/3}} \text{Ai}\left[-(t - z/c_{\text{gri}})/(q_0''' z/2)^{1/3}\right] e^{j(q_i z - \omega_i t)}, \qquad (2.2)$$

where ω_i is the inflection frequency, $c_{\text{gri}} = c_{\text{gr}}(\omega_i)$, $q_i = q(\omega_i)$, C is a constant, and Ai is the Airy function.

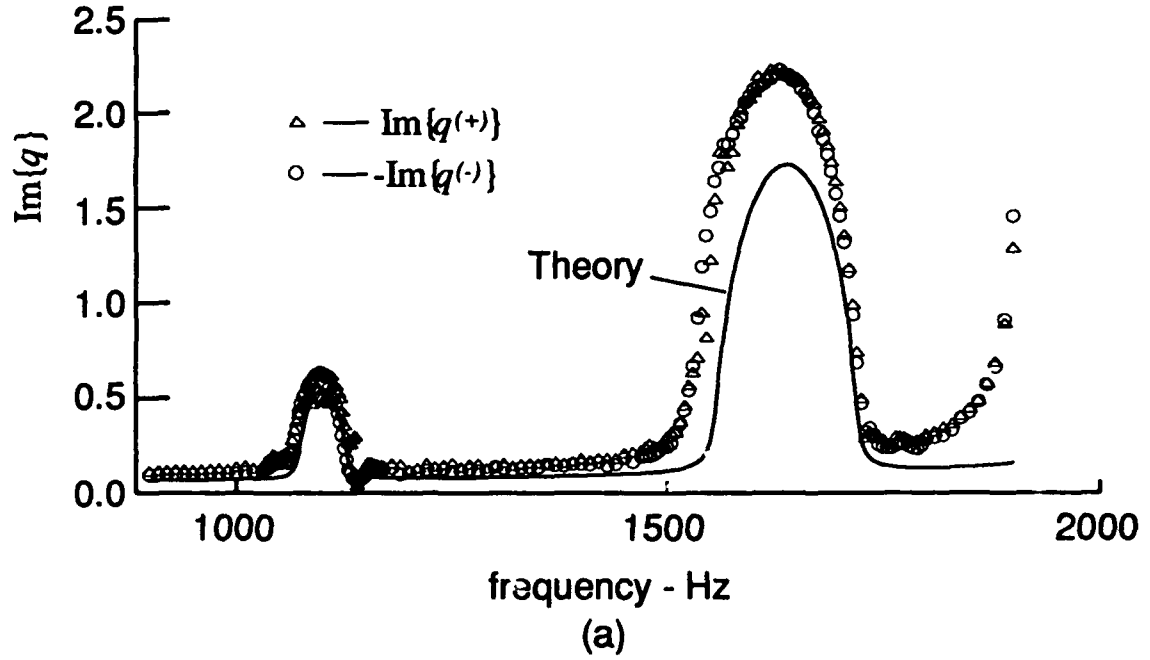

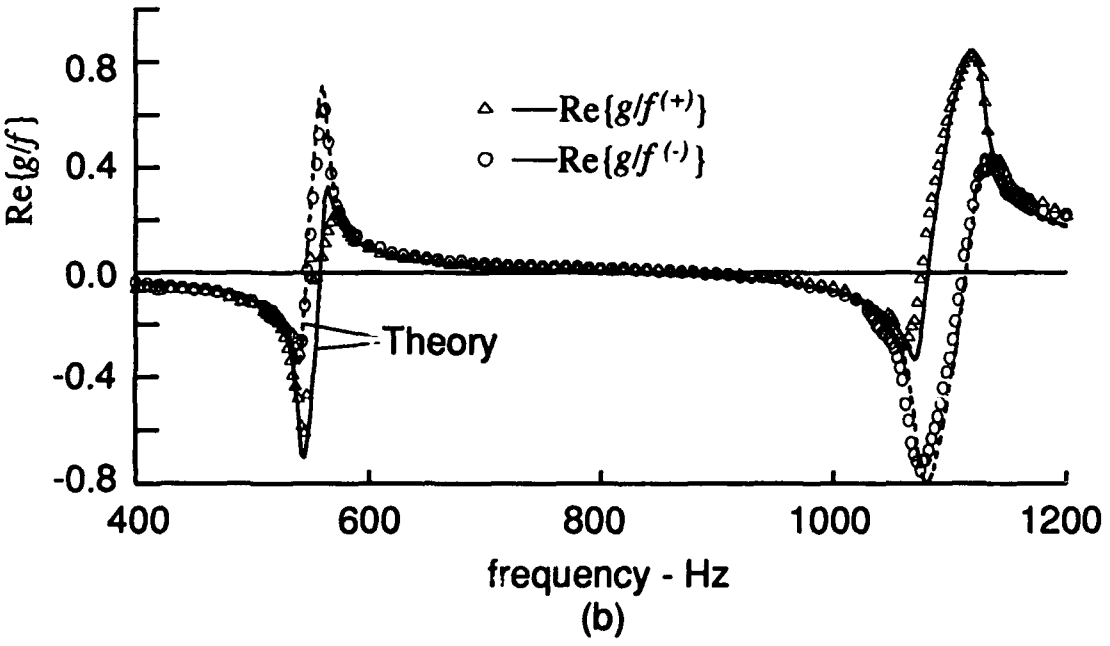

FIGURE 2.2
Theoretical and experimental values (a), of $\pm\mathrm{Im}\{q^{(\pm)}\}$, and (b) of $\mathrm{Re}\{g/f^{(\pm)}\}$.

AS-93-253

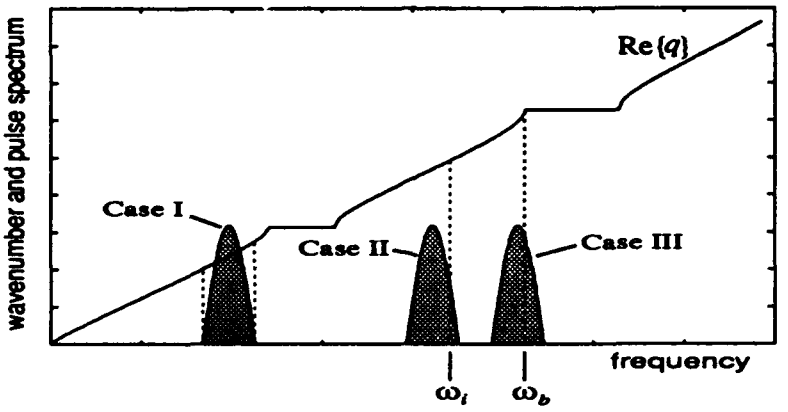

FIGURE 2.3
The relationship between the pulse spectrum and the dispersion curve for the three asymptotic solutions.

AS-93-254

III. The pulse spectrum includes a stop band boundary frequency ω_b. The asymptotic solution at any distance, but long after passage of the leading edge of the pulse, is

$$p(z,t) \sim Czt^{-3/2}F_{\text{env}}(\omega_b)e^{-j\omega_b t}. \tag{2.3}$$

The pulse has a long tail which oscillates at a frequency of ω_b and decays as $t^{-3/2}$.

It should be noted that Eqs. 2.1-2.3 are the solutions of the "analogous conventional wave problem", in which the periodic medium is treated as a conventional wave medium with the impedance and dispersion of the periodic medium. As was pointed out in last year's report (91-5), the solution of the periodic medium problem can be recovered from that of the analogous conventional wave problem via the operator $\psi(z) * \sum_n \delta(z - nh)$.

2.1.3 Nonlinear Bloch Wave Pulses

In order to make a simplified first pass at the problem of nonlinear Bloch wave pulse propagation, we make use of an earlier result from the nonlinear time harmonic Bloch wave propagation problem. It was found that a progressive, time harmonic fundamental Bloch wave results in a bidirectional excitation of second harmonic Bloch waves (90-3, 90-4, 90-7). As a first attempt to solve the nonlinear pulse problem, we

will consider only the second harmonic propagating in the same direction as the fundamental. While it is expected that the fundamental will generate a uniform backward traveling second harmonic Bloch wave that will stream steadily off the tail of the forward traveling fundamental pulse, the amplitude is expected to be very small. The reason for this is illustrated by the following argument. Consider a nondispersive wave system in which the fundamental pulse generates P_1 watts of forward traveling second harmonic and P_2 watts of backward traveling second harmonic. The generated forward traveling second harmonic will travel along with the fundamental and the power will be deposited into the same space-time region as the fundamental. This resonant deposition of power allows the forward traveling second harmonic to become quite concentrated. The backward traveling second harmonic, however, is traveling ~ 700 m/s relative to the fundamental, so any power will be smeared out over a very large region of space-time. This relatively diffuse deposition of power results in a very small wave amplitude.

We consider a semi-infinite periodic waveguide excited at the boundary according to $p(z,t)|_{z=0} = A(t)\cos(\omega_0^{(1)}t)$, where $A(t)$ is the envelope function. Up to the smallest characteristic envelope distortion distance (which is, as shown in last year's report (91-5), bandwidth dependent), the fundamental pulse has the form

$$p_1(z,t) = A(t - z/c_{\text{gr}}^{(1)})\cos(q_0^{(1)}z - \omega_0^{(1)}t).$$

Again, this solution, as well as the following second harmonic solutions, is that of the analogous conventional wave problem.

The forward traveling second harmonic solution has been found for a completely general case but, as usual, more physical insight is to be found in simpler cases. We consider two:

- Group synchrony case. The group velocities of the fundamental and the second harmonic are equal ($c_{\text{gr}}^{(1)} = c_{\text{gr}}^{(2)}$), but the phase velocities are not ($c_{\text{ph}}^{(1)} \neq c_{\text{ph}}^{(2)}$ or, equivalently, $q_0^{(1)} \neq q_0^{(2)}/2$). The second harmonic solution is

$$p_2(z,t) = \frac{\beta\omega_0^{(1)}}{2\rho_0 c_0^3}\left(\frac{\sin[(q_0^{(1)} - q_0^{(2)}/2)z]}{q_0^{(1)} - q_0^{(2)}/2}\right) A^2(t - z/c_{\text{gr}})\sin[(q_0^{(1)} + q_0^{(2)}/2)z - \omega_0^{(2)}t],$$

  where β is the coefficient of nonlinearity and c_0 is the free-medium sound speed associated with the fluid in the periodic waveguide. The second harmonic envelope, which propagates with the fundamental envelope, is simply the fundamental envelope function squared. The effect of the phase asynchrony is, as in the time harmonic case, a spatial beating of the envelope at intervals of $2\pi/(q_0^{(2)} - 2q_0^{(1)})$. Figure 2.4(a) shows the second harmonic envelope growing and decaying as the wave propagates.

- Phase synchrony case. The phase velocities are equal but the group velocities are not. The second harmonic solution is

$$p_2(z,t) = \frac{\beta\omega_0^{(1)}}{2\rho_0 c_0^3}\left(\frac{c_{gr}^{(2)}c_{gr}^{(1)}}{c_{gr}^{(2)} - c_{gr}^{(1)}}\right)\int_{t-z/c_{gr}^{(1)}}^{t-z/c_{gr}^{(2)}} A^2(\tau)d\tau \sin(q_0^{(2)}z - \omega_0^{(2)}t).$$

The second harmonic envelope is given by the integral term, which is simply the convolution of A^2 with a gradually widening rect function. As seen in Fig. 2.4 for the case $c_{gr}^{(1)} > c_{gr}^{(2)}$, the second harmonic energy is able to "leak out" of the region the fundamental pulse occupies. This sort of second harmonic behavior, which is not found in nondispersive systems, allows a second harmonic precursor to arrive at a receiver prior to the arrival of the fundamental pulse.

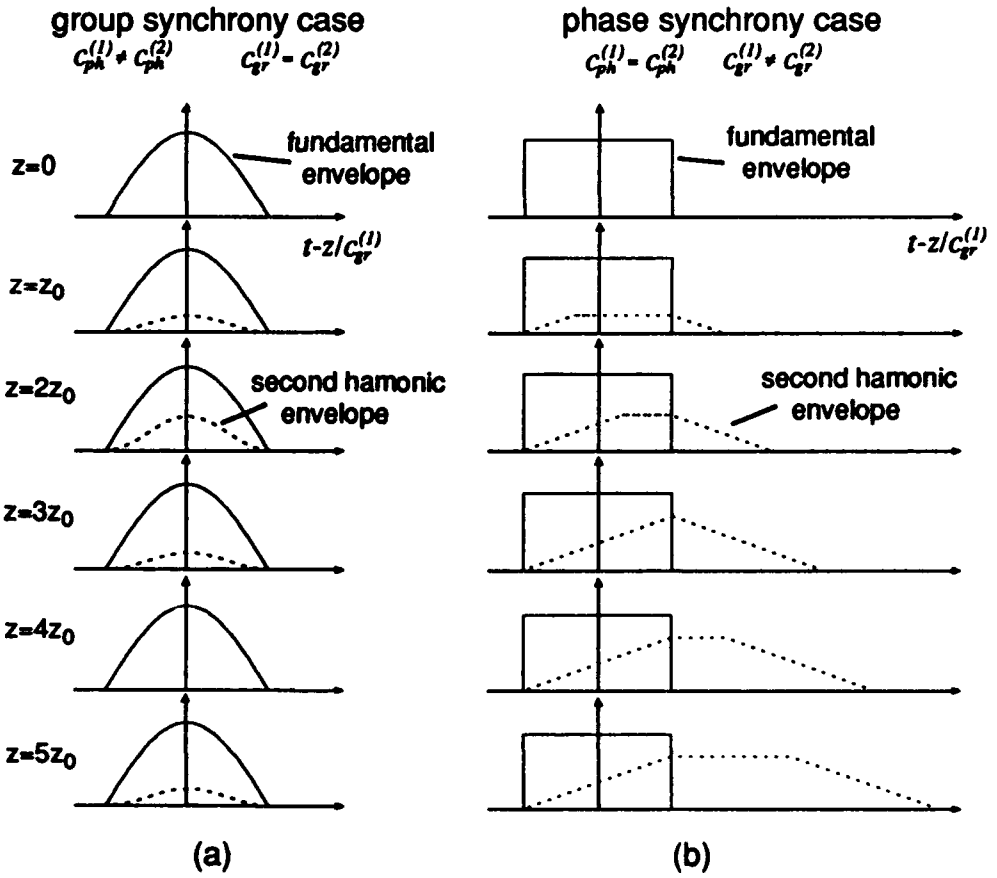

FIGURE 2.4
The fundamental and second harmonic envelopes for (a) the phase synchrony case and (b) group synchrony case.

AS-93-255

2.1.4 Group Velocity of Bloch Wave Pulses in the Stop Band

It was reported earlier (91-5) that the group velocity and the energy transport velocity generally differ for Bloch waves. One of the interesting differences occurs in the stop bands, where the energy transport velocity approaches zero and the group velocity becomes very large. To investigate, we constructed a system consisting of a section of uniform waveguide terminated in a section of periodic waveguide. Gaussian envelope pulses were launched towards the interface from the uniform waveguide side (see Fig. 2.5) and the acoustic pressure was recorded at various positions along the uniform waveguide, at the interface, and down the periodic waveguide. The set of time series shows the incident conventional wave pulse, the reflected conventional wave pulse, and the transmitted Bloch wave pulse. If the time series are laid out perpendicular to the z axis, each at the value of z corresponding to the measurement location, we get the characteristics-plane view illustrated in Fig. 2.5. The group velocity of the pulse is evident in the angle the pulse makes in the z-t plane. Note that for the example below, the transmitted Bloch wave pulse has a *slower* group velocity than the incident and reflected conventional wave pulses.

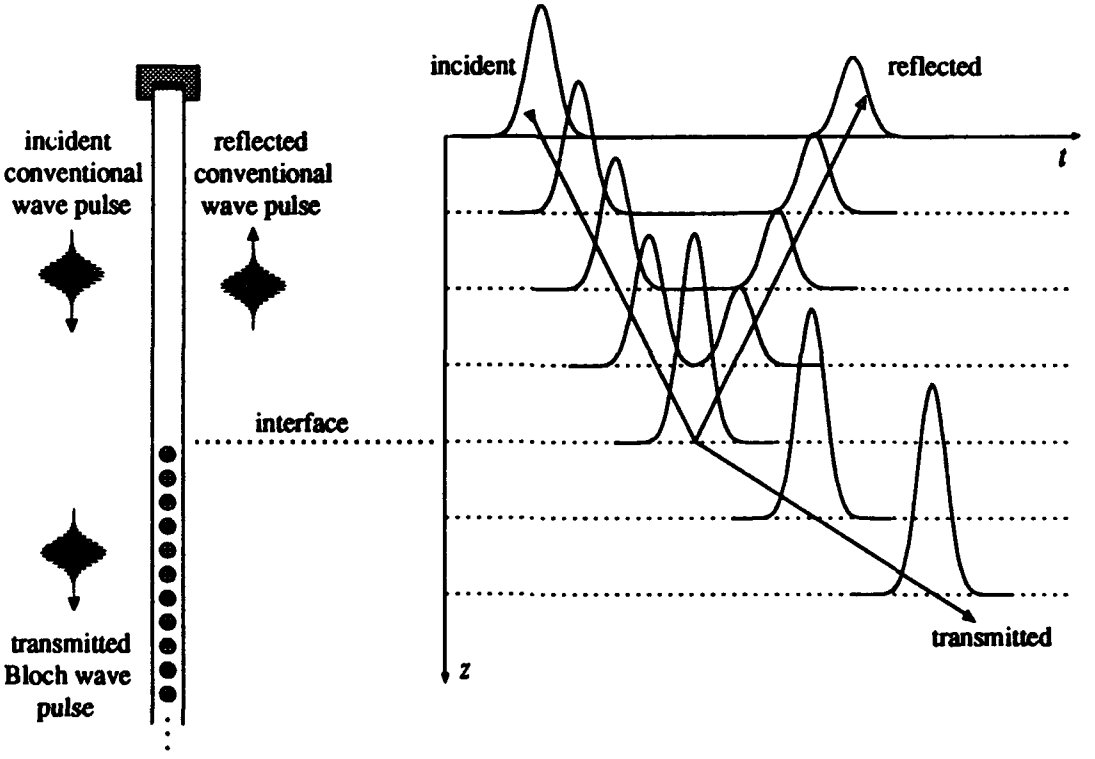

FIGURE 2.5
A set of time series arranged in characteristics form.

AS-93-256

Measurements were made at 3200 Hz (passband case) and at 1560 Hz (π stop band case). The set of time series from the passband case is shown in Fig. 2.6(a). The incident and reflected conventional wave pulses and the transmitted Bloch wave pulse are clearly evident. The group velocity of the transmitted pulse is slightly smaller than that of the incident and reflected pulses. Figure 2.6(b) shows the set of time series from the stop band case. While the transmitted pulse decays rapidly, its group velocity is nearly infinite. Figure 2.7 shows the very nearly simultaneous arrival of the pulse at all eight post-interface measurement locations.

This measurement graphically illustrates that near-infinite group velocities are indeed possible. When the issue is addressed in the literature, it is usually argued that in spectral regions where the group velocity becomes larger than the free-medium phase speed, the approximations involved in arriving at a meaningful definition of group velocity are violated.[2] That is, in a spectral range associated with large group velocity, the smallest characteristic pulse distortion distance (91-5) is small compared to a meaningful propagation distance. Before the pulse can propagate a distance comparable to its length, it is so badly distorted that the time of arrival of the pulse becomes ill-defined. Figure 2.7 shows, to the contrary, that very little distortion occurs. Indeed, at frequencies near the center of the stop band, the smallest characteristic pulse distortion distance can be arbitrarily large. The group velocity is indeed well-defined and, in some spectral regions, much larger than c_0. While they are intriguing, these supersonic pulses are of purely academic interest as they only exist at stop band frequencies and therefore attenuate rapidly.

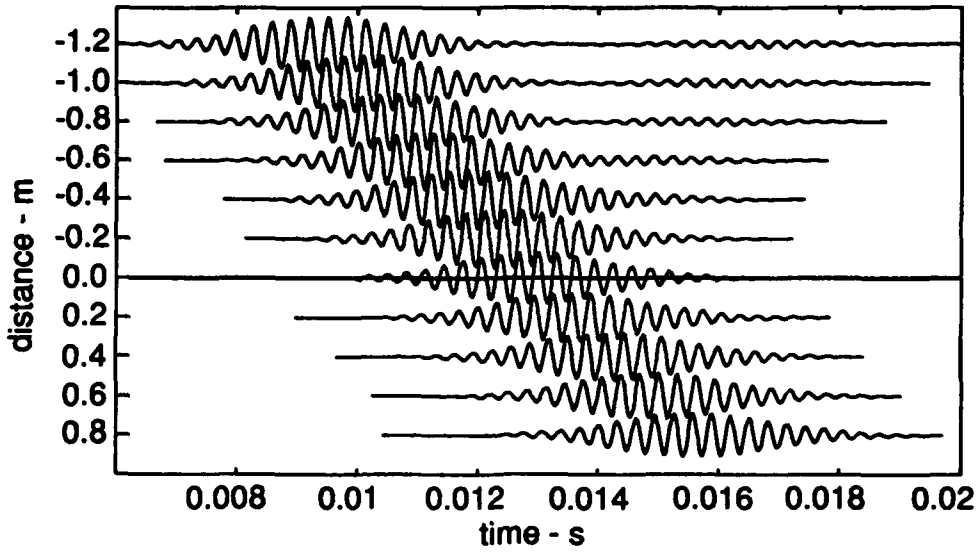

(a) 3200 Hz (passband)

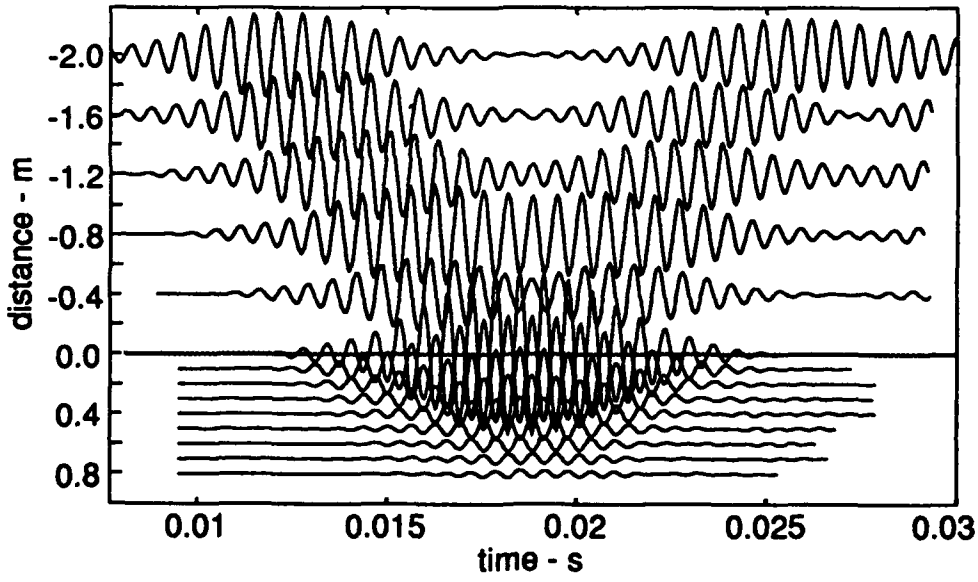

(b) 1560 Hz (stop band)

FIGURE 2.6
Measured time series arranged in characteristics form for Gaussian pulses with carrier frequencies of (a) 3200 Hz (passband) and (b) 1560 Hz (stop band).

AS-93-257

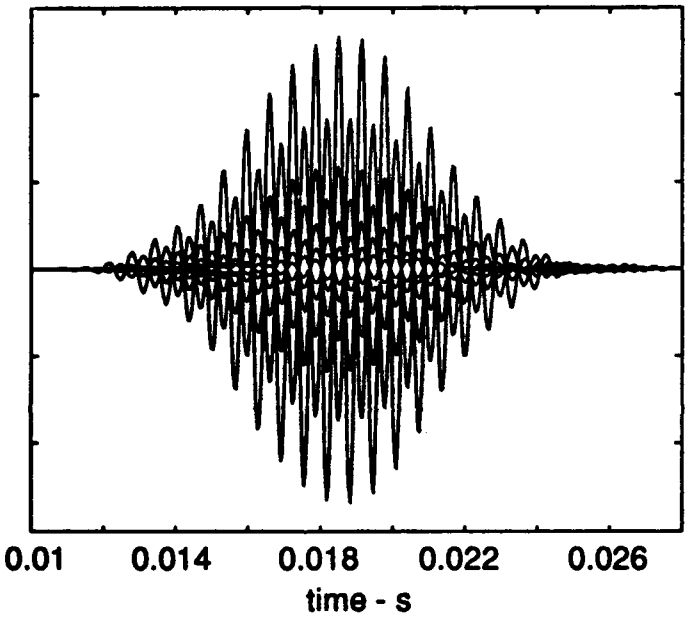

FIGURE 2.7
The eight post-interface time series for the 1560 Hz carrier (stop band) case. AS-93-258

2.2 Scattering of Sound by Sound

Except for publication of Ten Cate's dissertation (92-2) as a technical report and publication of one or more journal articles about the work, this project is now complete. Refer to the previous two annual reports[1,3] (91-5, Sec. 2.2, and 90-4, Sec. 2-2) for figures showing key theoretical and experimental curves. The following material is adapted from Chap. 4 of Ten Cate's dissertation, Summary and Conclusions.

Ten Cate's research, which was primarily experimental, sheds light on a classic, yet controversial, problem in nonlinear acoustics, the scattering of sound by sound. No one doubts that secondary sound is *produced* from the nonlinear interaction of two sound beams. Whether the secondary sound is *scattered* or *radiated* outside the region of interaction has, however, been the subject of a great deal of controversy. New theoretical work by the Tjøttas and their coworkers resulted in a series of papers beginning in the mid-1980s[4-8] that provided a fresh perspective on the problem of scattering of sound by sound. Armed with the insights provided by these papers, Ten Cate performed a new set of experiments.

Chapter 1 begins with a reexamination of the origin and history of the scattering of sound by sound. What was meant by "scattering of sound by sound" in the early 1950s is different from what is meant now. Originally the term signified secondary components resulting from the nonlinear interaction of two crossed sound beams of different frequency. Recently the "definition" has been expanded to include part of the nonlinearly generated sound — called *fingers* — produced in a single beam (single source excited at a single frequency). Ten Cate thus designed experiments to measure two types of scattered sound: self-scattering in single beams, and classical crossed-beam scattering. Chapter 1 concludes with a careful review of earlier experiments, including both types of scattering, with comments about what can be learned from them.

The theory necessary to understand the scattering of sound by sound is presented in Chap. 2. Two theoretical approaches are highlighted: the KZK (Khokhlov-Zabolotskaya-Kuznetsov) equation for self-scattering, and a generalized Westervelt equation for classical crossed-beam scattering. A numerical algorithm developed by the Bergen group[9-12] for solving the KZK equation is briefly described and explained. The generalized Westervelt equation, especially its quasilinear version, is then discussed. A known asymptotic solution,[7] for which numerical evaluation is required,[8,13] is given special attention because of its application later to some of the experiments.

The experimental measurements are reported in Chap. 3, for both kinds of scattering. In order to put the measurements into perspective, we begin with some background information. Self-scattering is taken up first.

Scattered sound in the form of fingers (extra sidelobes) in the higher harmonic beam patterns measured for a uniform piston source (single beam) has been seen before. In fact, although they were not explained at the time, fingers can be identified in measured beam patterns published as early as 1966.[14] Fingers were not recognized as scattered sound until the mid-1980s when accurate numerical solutions of the KZK equation became practical.[4] Calculated beam patterns then began to provide a good explanation of the earlier measurements.[4,10] Until Ten Cate's research, however, no one had *carefully* measured beam patterns and compared them with theory, particularly beyond the second harmonic. Nor had any specific attempt been made to measure propagation curves for the finger radiation. The first half of Chap. 3 is devoted to Ten Cate's experiments on self-scattering. His measurements, which include beam patterns for the first ten harmonics, are compared in detail with predictions obtained from numerical solution of the KZK equation. Agreement is excellent. Measured propagation curves confirm that the fingers decay as $1/r$ (when thermoviscous absorption is factored out) whereas the other sidelobes decay more slowly. Taken as a whole, the measurements clearly identify fingers as scattered sound (91-7).

Crossed-beam scattering of sound by sound experiments have been performed since the mid-1950s, and arguments about the existence of scattered sound continue to this day. In contrast to some earlier researchers, the Tjøttas and their coworkers showed that it should be possible to observe scattering of sound by sound in a crossed-beam experiment.[8] The Tjøttas' predictions were supported by an analytical solution of the KZK equation by Darvennes and Hamilton[15] for Gaussian beams. After many numerical simulations, Ten Cate came up with a few rules of thumb for observation of scattered sound. The rules of thumb were used to design the crossed-beam experiments that are reported in the latter half of Chap. 3. Unfortunately, the results of these experiments are at best only inconclusive.

The ideal crossed-beam experiment would be done with Gaussian sources because no ordinary (product pattern) sidelobes would be present to interfere with observation of the scattered sound. Since only one Gaussian source could be obtained (and it was really only a shaded source, not truly Gaussian), Ten Cate performed several experiments with it and an ordinary uniform piston. No scattered sound was observed. Failure is not deemed significant, however, because the quality of the Gaussian source was poor. The radiation was neither symmetric nor free of sidelobes. Because of this, it was impossible to obtain a reliable theoretical prediction of the level of the expected scattered sound. A second set of crossed-beam experiments was then performed, this time with two uniform sources. Because the primary beams were replete with sidelobes, however, a useful theoretical prediction was again impossible. Moreover, the very large amount of product-pattern sum and difference frequency radiation, which is due to the sidelobes in the primary radiation and is *not* scattered sound, made it very difficult to detect true scattered sound, which is expected to be weak. Some evidence of scattered sound was nevertheless obtained in the form of deviations

from product-pattern radiation at the sum and difference frequencies.

The conclusions from Ten Cate's study are thus as follows. (1) Self-scattering is now very well understood. Nearfield effects, which are included in the KZK theoretical model, give rise to finger radiation. Predictions based on the KZK model are in excellent agreement with experimental data. Fingers have also been shown to fit the present day "definition" of scattered sound. (2) Classic scattering of sound by sound is also fairly well understood. Ten Cate's crossed-beam experiments, however, neither confirm nor deny the presence of scattered sound. Part of the difficulty is theoretical in that reliable predictions are not yet available for sources as complicated as Ten Cate had to use. The recommended cure is not, however, to develop a more robust theory but rather to perform the experiment with two truly Gaussian sources. Only then will it be possible to avoid competition from product-pattern radiation.

2.3 Finite-Amplitude Waves in a Three-Layer Fluid

The construction and initial testing of the high precision positioning system was completed early in the report period. Figure 2.8 gives a diagram and sketch of the system, in this case, as used for an experiment with the water tank in the present project. The National Instruments LabVIEW interface allows users of the system to combine data acquisition and position control (just as is done with the system in the Mechanical Engineering Department on campus). Since its completion, the system has been used extensively in two experiments: (1) aperture diffraction of a pulse produced underwater by a spark (see Sec. 2.5 below), and (2) propagation of airborne N-waves through a turbulent jet (work done under a NASA grant).

Investigation of propagation of sound through multiple media was begun with a study of finite-amplitude waves incident on a metal plate contained in a water bath. The study is guided by the work of V. E. Nazarov[16] who describes a novel method for measuring the acoustical nonlinearity parameter β in a medium.

Figure 2.8 shows the arrangement of the transducer and metal plate used. The lossless wave equation in Lagrangian coordinates[17] is used to describe the wave motion in terms of the particle displacement ξ, the rest position x, the small-signal sound speed c_0, and the coefficient of nonlinearity β:

$$\xi_{tt} - c_0^2 \xi_{xx} = -2\beta c_0^2 \xi_x \xi_{xx} \quad . \tag{2.4}$$

The source pressure is given by

$$p_{\text{source}} = A \sin \omega t \quad , \tag{2.5}$$

and the field consists of incident, reflected, and transmitted waves in the water and a standing wave field in the plate. Because of nonlinear effects in the plate and the

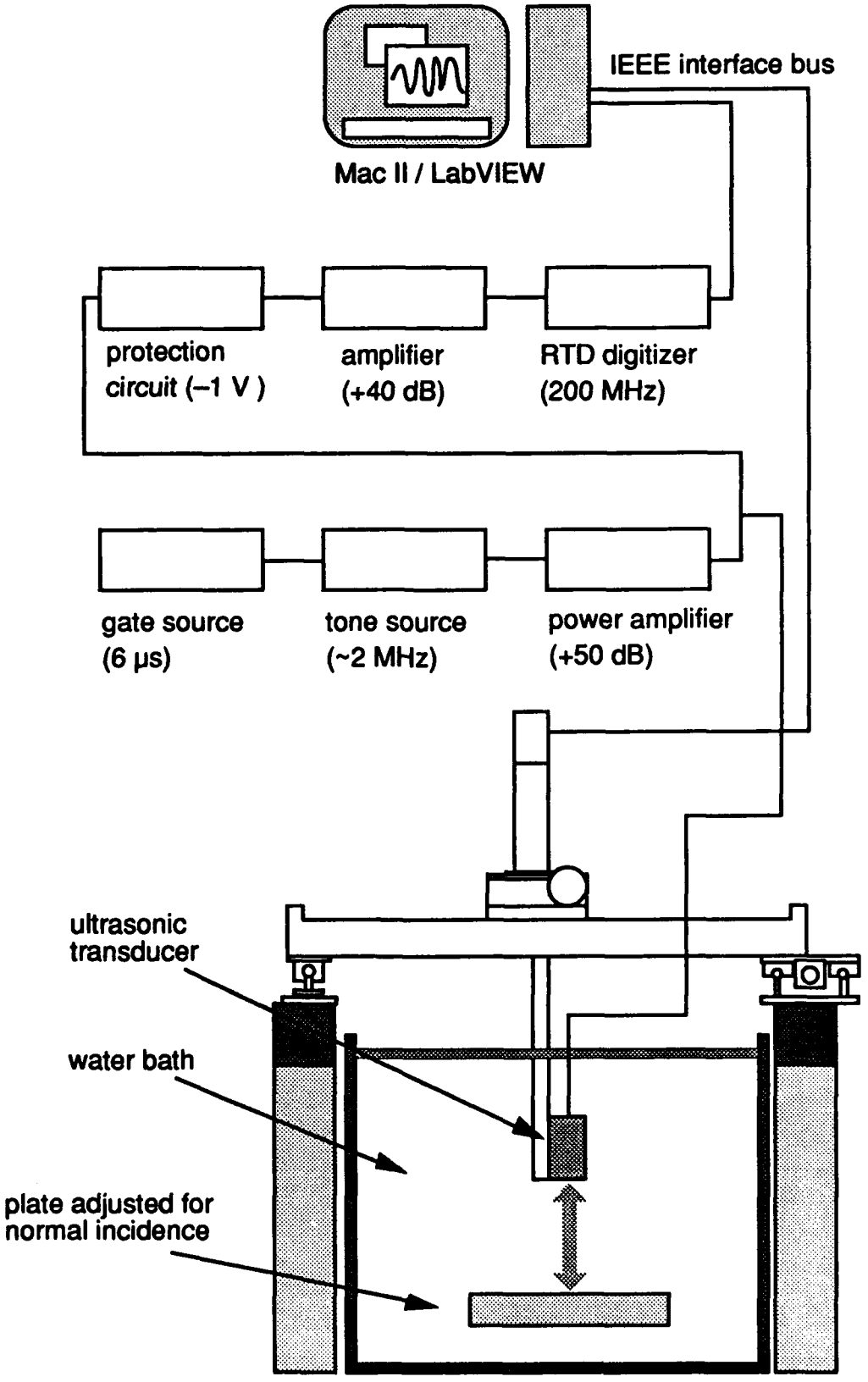

FIGURE 2.8
Positioning system and tank for three-medium experiment.

AS-93-259

water, second and higher harmonics are present in addition to the fundamental. In what follows, p_1 and p_2 are the amplitudes of the fundamental and second harmonic, respectively; ρ_0, c_0, k_0, and β_0 refer to properties of the plate, while unsubscripted quantities refer to properties of the water.

If the frequency of the source is selected so that the thickness of the plate L_0 is an integral number of half-wavelengths in the plate, i.e.,

$$L_0 = \frac{n\pi}{k_0} \quad , \tag{2.6}$$

then the fundamental and higher harmonic signals incident on the plate should be

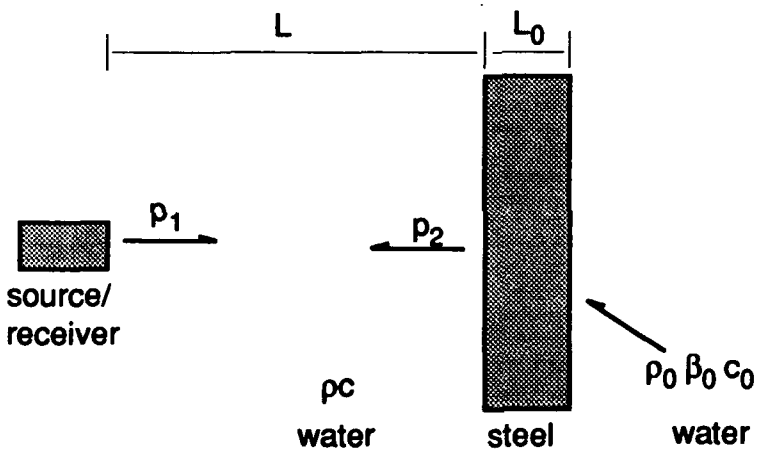

FIGURE 2.9
Arrangement of plate in water. AS-93-260

perfectly transmitted through it. Higher harmonics generated in the plate should, however, be radiated into the left and right half spaces. Using the perturbation method and applying the boundary conditions at the interfaces, we obtain the following expression for the second harmonic radiated back toward the source:

$$p_2 = \frac{\pi n}{8}\beta_0 \frac{A^2[1 - \left(\frac{\rho c}{\rho_0 c_0}\right)^2]}{\rho c c_0} \quad . \tag{2.7}$$

Therefore, if A and p_2 are measured, the coefficient of nonlinearity β_0 of the plate can be determined.

A test of the method in the form of an experiment has been started. The positioning system described above is used to align an ultrasonic transducer (Ultran

Laboratories 2.2 MHz, 3 mm radius) and an aluminum plate ($L_0 = 1.2$ cm) as shown in Fig. 2.9. The experimental setup is shown in Fig. 2.8. A tone burst of 20 μs is used in order to resolve the incident and reflected waves. The source voltage is 150 V p-p. The signal is digitized at 200 MHz using the RTD and transferred to the LabVIEW program. A Hamming filter is used to minimize the effects of the tone gate, and the Fourier transform (FT) is obtained. The FT is averaged about 100 times to increase the dynamic range of the measurements. Estimates indicate that the level of the re-radiated second harmonic should be about 60 dB below that of the source. Preliminary results show a difference of about 50 dB.

2.4 Finite-Amplitude Propagation in a Medium Having a Distribution of Relaxation Processes

This research began in 1990 with support from a NIH grant. Although the work did not become a project under the present ONR grant until 1 September 1991, for continuity the carlier work is reviewed here along with the progress made during the current year.

Emphasis during the period of NIH support was on the absorption of high intensity ultrasound by tissue. Nonlinear propagation effects, whether the ultrasound is used for diagnosis or diathermy, can greatly increase absorption of the ultrasound by the tissue irradiated.[18] The medical consequence is a greater rise in tissue temperature than would have been expected on the basis of linear theory. The absorption α may be defined in terms of the intensity I of the ultrasound; for plane waves the relation is

$$\alpha_f = -\frac{dI/dx}{2I} \quad , \tag{2.8}$$

where the subscript f has been used to emphasize our interest in finite-amplitude absorption (the symbol α_0 denotes small-signal absorption). For nonplanar waves dI/dx is replaced by the divergence of the intensity.

Our first approach was to use weak-shock theory and make the calulation of α_f in the time domain. The result was a closed form prediction of α_f for a variety of different waves.[19] Our work complemented that of Carstensen *et al.*,[18] who used a frequency domain method, which led to Fourier series that had to be summed numerically. Li's first work on the problem was to include the effect of ordinary absorption* for a plane finite-amplitude wave that is sinusoidal (angular frequency ω) at its source. He used Burgers' equation (see Eq. 2.9 below) and applied its known solution[20] to calculate the absorption. This work was completed in 1990 and is reviewed in Sec. 2.4.1 below.

*When weak shock theory is used, the only absorption accounted for is that associated with shocks in the waveform.

Although the results were interesting in that they filled in the gaps where weak-shock theory fails, i.e., before shocks form and after they become very weak, Burgers' equation is valid only for a thermoviscous fluid, which is not a good model for most tissues. Thermoviscous fluids have negligible dispersion and a small-signal absorption α_0 that varies as ω^2. By contrast, experiments show that most tissues at frequencies in the MHz region are dispersive and have absorption that is proportional to ω^n, where n has a value very close to unity† (the range is 1 to about 1.2). The derivation of a generalized Burgers equation,[21] or GBE (Sec. 2.4.2), for tissue thus began to occupy Li's attention early in 1991. Using the model of tissue as a medium with a continuous distribution of relaxations,[22] he obtained a nonlinear integro-differential equation as the GBE for this case (see Sec. 2.4.2). Attempts to obtain solutions came next. He first developed a stationary solution, that is, the solution for a steady shock wave (Sec. 2.4.3). More recently he has attempted a solution for a wave sinusoidal at the source (Sec. 2.4.4). ONR support of the project began with the results given in Secs. 2.4.3 and 2.4.4.

2.4.1 Finite-Amplitude Absorption for Thermoviscous Fluids

Propagation of finite-amplitude waves in thermoviscous fluids is described by the classical Burgers equation,

$$u_x - bu_{t't'} = (\beta/c_0^2)uu_{t'} \quad , \tag{2.9}$$

where u is particle velocity, x is distance from the source, $t' = t - x/c_0$ is retarded time (t is actual time), c_0 is small-signal sound speed, β is the coefficient of nonlinearity, and b is proportional to the coefficients of viscosity and heat conduction (the small-signal absorption is given by $\alpha_0 = b\omega^2$). A convenient dimensionless form of Burgers' equation is

$$v_\sigma - \frac{1}{\Gamma} v_{yy} = vv_y \quad , \tag{2.10}$$

where $v = u/u_0$ is the dimensionless particle velocity, u_0 is a characteristic particle velocity of the physical system, say the source amplitude, $y = \omega t'$ is the dimensionless retarded time, $\sigma = x/x_s$ is distance relative to the shock formation distance $x_s = c_0^2/\beta u_0 \omega$, and $\Gamma = (\alpha_0 x_s)^{-1}$. The physical significance of Γ is that it is a measure of the importance of nonlinearity relative to dissipation. For periodic waves Eq. 2.10 may be used to reduce Eq. 2.8 to

$$\alpha_f = \alpha_0 \frac{\int_0^{2\pi} v_y^2 \, dy}{\int_0^{2\pi} v^2 \, dy} \quad . \tag{2.11}$$

†The absorption characteristic for tissue is thus quite similar to that for porous matter such as marine sediments. This implies that Li's work may have application to finite-amplitude propagation in sediments.

The expression for v is known from the exact solution of Burgers' equation.[20] Equation 2.11 may therefore be evaluated, although in practice the evaluation must be done numerically. Typical curves for finite-amplitude absorption for relatively weak waves — $\Gamma = 2, 5, 10$ — are shown in Fig. 2.10. The small departure of the curve for $\Gamma = 2$ from the linear theory prediction shows that the wave in this case is very nearly a small signal. The curves for $\Gamma = 5$ and 10, however, show that nonlinear effects can cause a substantial increase in the absorption. Put another way, the linear theory prediction is only adequate (1) very near the source, where harmonic distortion is still small, and (2) very far from the source, where most of the harmonic distortion components have damped out and a sinusoidal waveform has been virtually restored. In between, the birth of shocks and the establishment of a sawtooth (at least for $\Gamma = 10$) greatly increases the efficiency of the absorption process.

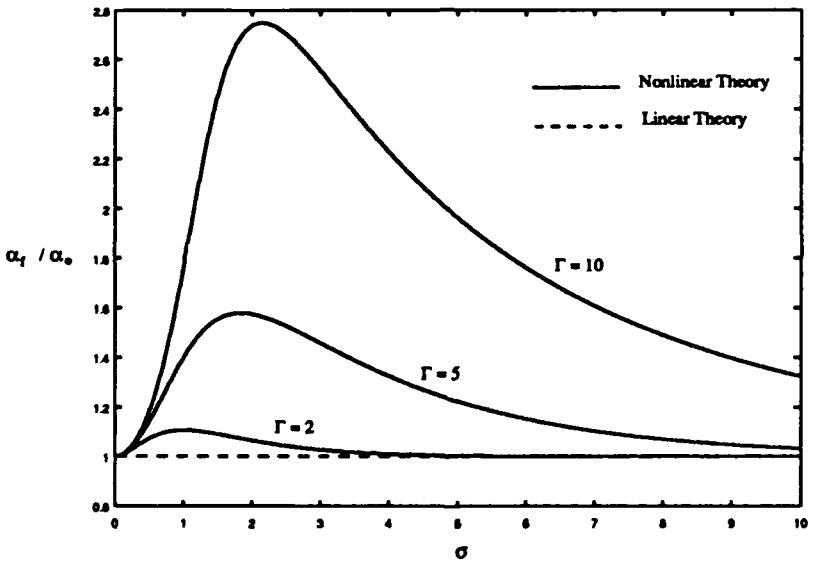

FIGURE 2.10
Finite-amplitude absorption as a function of distance for a thermoviscous fluid, $\Gamma = 2, 5, 10$.

AS-93-261

It is interesting to compare the present results with those obtained by using weak-shock theory, which, as has already been noted, is a theory based on the assumption that absorption is due solely to whatever shocks are present in the waveform. Figure 2.11 is a repeat of Fig. 2.10 but with curves for weak-shock theory predictions added. Several observations may be made. First, because no shocks are present in the region $0 < \sigma < 1$, the weak-shock model gives $\alpha_f = 0$ there. Second, for $\Gamma = 2$ the failure of the weak-shock curve to get even close to the linear theory prediction is further evidence of the insignificance of nonlinear effects for that case. It is clear that

as Γ increases, the predictions based on weak-shock theory become more realistic. Indeed, one finds that for high values of Γ, for example, $\Gamma > 100$, the weak-shock and Burgers equation predictions coincide over a large range. Third, the rather curious result that the weak-shock curve for $\Gamma = 10$ actually *exceeds* the corresponding Burgers equation curve may be explained as follows. Under the weak-shock assumption the wave amplitude does not decay until σ exceeds $\pi/2$. In the more realistic Burgers equation model, however, ordinary absorption combined with nonlinear distortion causes a reduction of the amplitude beginning at the source. Since α_f depends strongly on amplitude, the weak-shock theory overestimate of amplitude in the region near $\sigma = \pi/2$ causes the absorption to be overestimated there as well. Finally, it should be noted that one cannot arrive at the correct prediction for finite-amplitude absorption (represented by the Burgers equation curves) simply by adding the absorption due to ordinary losses to that due to shock losses. The interaction between ordinary dissipation and nonlinear distortion is too complicated to permit superposition. It should be noted that the method recently proposed by Dalecki *et al.*[23] for combining the two absorptions does not amount to superposition; some account of interaction is taken.

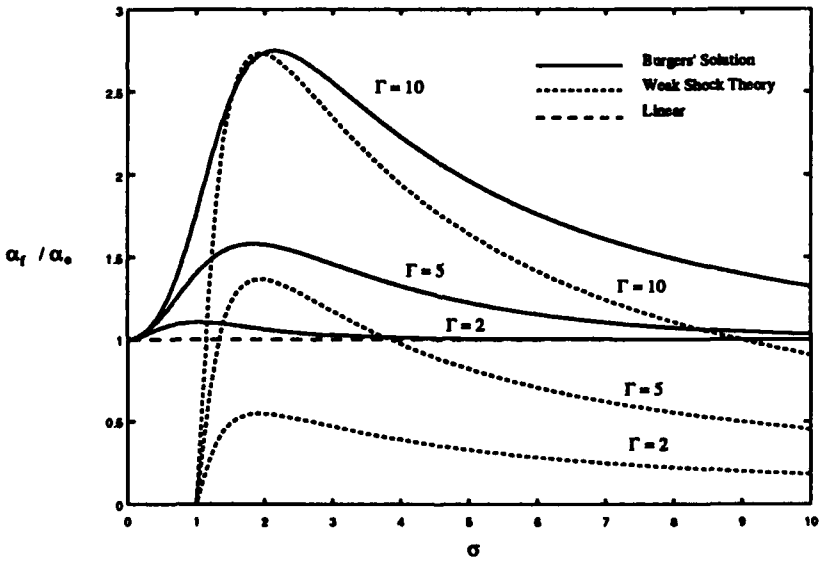

FIGURE 2.11
Plot of α_f/α_0 for $\Gamma = 2, 5, 10$ for three different models: Burgers' equation (——), weak-shock theory (- - -), and linear theory (– – –).

AS-93-262

Note that the method based on Burgers' equation is not restricted to waves that are sinusoidal at the source. Calculations may also be made for pulses. Moreover,

the evaluation of Eq. 2.11 may be done with either time domain or frequency domain expressions. The main drawback to the use of Burgers' equation is its restriction to plane waves in thermoviscous fluids. The method is, however, very useful for the physical insight it provides about the roles of shocks and ordinary losses in producing the total absorption.

2.4.2 A Generalized Burgers Equation for Tissue

When the medium cannot be characterized as thermoviscous, that is, when the dispersion is not negligible and α_0 is not proportional to ω^2, it is still possible to develop a Burgers-like equation, called a "generalized Burgers equation," or GBE.[21] Li derived a GBE for tissue. Before presenting the results of this derivation, however, we first give some background.

The form of the generalized Burgers equation given by Blackstock[21] is

$$u_x + L[u] = \frac{\beta}{c_0^2} u u_{t'} \quad , \tag{2.12}$$

where $L[u]$ is a linear operator that describes the (small-signal) absorption and dispersion properties of the fluid. For example, for a thermoviscous fluid $L[u] = -bu_{t't'}$. Let the absorption and dispersion properties be specified in terms of a function ζ,

$$\zeta(\omega) = \alpha_0(\omega) - j\delta(\omega) \quad , \tag{2.13}$$

where δ is the dispersion function

$$\delta(\omega) = \omega(1/c_0 - 1/c_{\text{ph}}) \quad ,$$

and it is assumed that both α_0 and δ are known functions, either from experimental measurements, theoretical considerations (including the Kramers-Kronig relation), or both. Li developed the following general expression for $L[u]$ in terms of ζ:

$$L[u] = \frac{1}{\sqrt{2\pi}} \int_{-\infty}^{\infty} dt'' u(x, t'') K(t' - t'') \quad , \tag{2.14}$$

where the kernel K is the inverse Fourier transform of the absorption-dispersion function ζ,

$$K(t) = \frac{1}{\sqrt{2\pi}} \int_{-\infty}^{\infty} d\omega \zeta(\omega) e^{j\omega t} \quad . \tag{2.15}$$

For example, for a thermoviscous fluid $\zeta = b\omega^2$, and the kernel becomes proportional to the second derivative of the dirac delta function. Equation 2.14 then reduces to $-bu_{t't'}$ and the classical Burgers equation, Eq. 2.9, is recovered. The next task is to find the kernel function for tissue.

Propagation in tissue, which is generally dispersive, is quite different from that in thermoviscous fluids. For a discussion of the complicated mechanisms involved, see, for example, Jongen *et al.*,[24] who concluded that relaxation is the dominant process. The Carstensen-Schwan model, although originally proposed to describe the absorption and dispersion characteristics of hemoglobin,[22] has since been applied with success to a wide variety of tissues. Carstensen and Schwan took hemoglobin to be a medium having many relaxation processes, each having its own particular relaxation (angular) frequency Ω. Not having information about each relaxation, they assumed that the collection of discrete processes could be represented by a continuous distribution of relaxation processes in the range $\Omega_1 < \Omega < \Omega_2$. Accordingly, the total absorption was expressed as an integral from Ω_1 to Ω_2 of $\alpha_0(\Omega)$, multiplied by a distribution (or weighting) function. They found that by choosing a distribution function proportional to $1/\Omega$ they obtained a good fit to the experimental data (α_0 proportional to ω over a wide band). Evaluation of the integral leads to the following expression for the total relaxation contribution (we omit here the viscosity contribution, which was included by Carstensen and Schwan):

$$\alpha_0(\omega) = M\omega(\arctan\omega\tau_L - \arctan\omega\tau_S) \quad , \tag{2.16}$$

where $\tau_L = 1/\Omega_1$ and $\tau_S = 1/\Omega_2$ are the largest and smallest relaxation times, respectively, in the distribution, and M is a constant proportional to the strength of relaxation, which can be determined experimentally. Similar treatment of the dispersion leads to

$$\delta(\omega) = \frac{M\omega}{2}\ln\left(\frac{1+\omega^2\tau_L^2}{1+\omega^2\tau_S^2}\right) \quad . \tag{2.17}$$

Evaluation of Eq. 2.16 shows the following. The distribution of relaxation mechanisms produces an absorption that is proportional to ω^2 for low frequencies ($\omega\tau_L \ll 1$), is equal to a constant for high frequencies ($\omega\tau_S \gg 1$) and, provided the distribution is wide enough ($\Omega_2 \gg \Omega_1$), is proportional to ω for the broad midfrequency range $\Omega_1 \ll \omega \ll \Omega_2$. The corresponding dependence of the dispersion, as given by Eq. 2.17, is $\delta \sim 0$ as $\omega \to 0$, while $\delta \sim \omega$ as ω becomes very large. In the midfrequency region the behavior is $\delta(\omega) \sim \omega\ln\omega$.

Substitution of Eqs. 2.16 and 2.17 in Eq. 2.13 leads to the following GBE (written in dimensionless form) for a medium having a distribution of relaxation processes:

$$v_\sigma - D\frac{\partial}{\partial y}\int_{-\infty}^{y} dy' v_{y'}(\sigma, y')K(y-y') = vv_y \quad , \tag{2.18}$$

where the kernel is given by

$$K(y) = \int_{y/\omega\tau_L}^{y/\omega\tau_S} \frac{e^{-\nu}}{\nu} d\nu \quad . \tag{2.19}$$

The important parameter $D = Mc_0/\beta\epsilon_0$ is a measure of the importance of dispersion relative to that of nonlinearity and thus plays a role similar to that played by $1/\Gamma$ for thermoviscous fluids.

If the range of the distribution is very narrow, that is, if $\tau_L \rightarrow \tau_S$, Eq. 2.18 reduces to the well known GBE for a medium having a single relaxation process.[25] Agreement for this case helps establish the credibility of Eq. 2.18. On the other hand, the implication is that prospects for an easy solution of Eq. 2.18 are not good. Since no general analytical solution is known for the single relaxation medium, an analytical solution of Eq. 2.18 is not to be expected either. Li has, however, attempted to find asymptotic solutions, a stationary solution, and some numerical solutions.

This subsection concludes with a brief account of the search for asymptotic solutions. First, Eq. 2.18, a nonlinear integro-differential equation, was converted to completely differential form. The resulting equation contains a logarithmic differential operator, which can be expressed as an infinite series of differentiations of increasing order. In the limit as $\omega \ll \Omega_1$, only the lowest term in the series is important, and the equation reduces to the classical Burgers equation, that is, Eq. 2.9. We thus confirm that for very low frequency disturbances, the relaxation mechanism is (as expected) frozen, and the tissue just behaves as a thermoviscous medium. If the source frequency is a little larger, so that the next term in the series must be included, the so-called Korteweg-deVries-Burgers equation is obtained. Although Li has not attempted a solution of this equation, it is known to be a good model for simple absorption and dispersion of finite-amplitude waves. For example, the effect of relaxation has been found to be responsible for the formation of weak pulsations occurring at the vertex of sawtooth waves.[26] We now proceed to results obtained during the period covered by this report.

2.4.3 Stationary Solution

After a wave equation for finite-amplitude disturbances in a new or novel medium has been developed, usually one of the first tasks is to attempt a steady shock, or stationary, solution of the equation. The steady shock is physically interesting because it shows in the most elementary way the balance, if one exists, between finite-amplitude distortion and dissipation. Moreover, it poses one of the simplest mathematical problems, since "stationary" means that the wave shape does not change with propagation distance. In the case of Eq. 2.18, dropping the spatial derivative term allows one to integrate the equation once with respect to y and obtain

$$v^2 = 1 - 2D \int_{-\infty}^{y} dy' v_{y'}(y') K(y - y') \quad ,$$

where the constant was found by requiring that $v \rightarrow \pm 1$ as $y \rightarrow \pm\infty$. For a steady shock, therefore, Eq. 2.18 reduces to an ordinary integral equation. Even so, the reduced equation is not easy to solve. Li has used the method of multiple scales to obtain a solution in the form of a perturbation series, as follows:

$$v = v_0 + \mu v_1 + \mu^2 v_2 + \cdots \quad , \tag{2.20}$$

where

$$v_0 = \tanh\chi$$

$$v_1 = -(1+r)\mathrm{sech}^2\chi \ln\cosh\chi$$

$$v_2 = -\mathrm{sech}^2\chi[4a_1^2(\tanh\chi \ln^2\cosh\chi + \tanh\chi \ln\cosh\chi - \tfrac{3}{2}(\chi - \tanh\chi)) + 4a_2(\chi - \tfrac{3}{2}\tanh\chi)]$$

$$\mu = [2D(1-r)]^{-1}$$

$$\chi = \mu y/\omega\tau_L$$

$$a_1 = (1+r)/2$$

$$a_2 = (1+r+r^2)/3$$

$$r = \tau_S/\tau_L = \Omega_1/\Omega_2 \quad .$$

The perturbation series converges rapidly if $\mu \ll 1$.

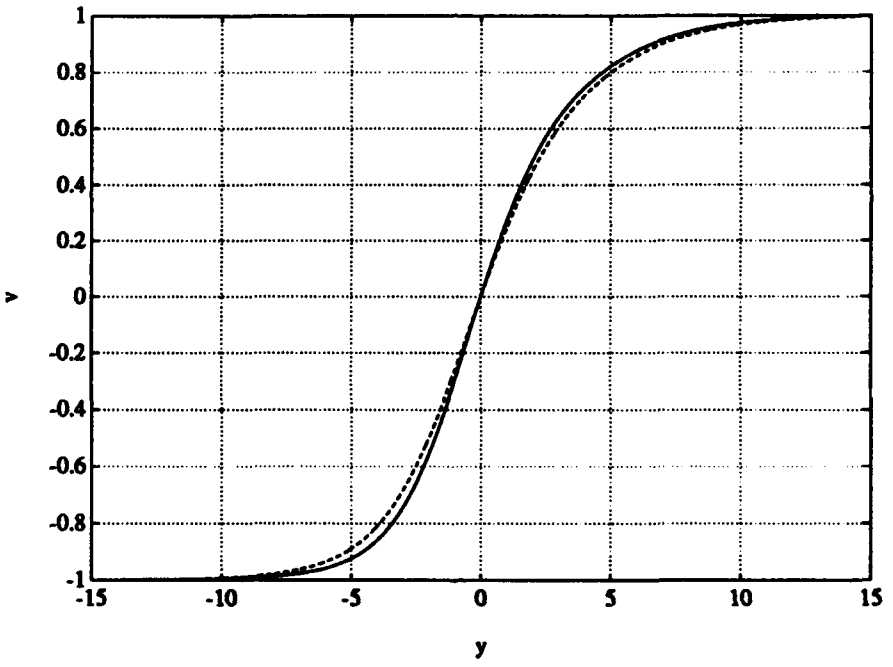

FIGURE 2.12
Profile of a steady shock in a medium having a distribution of relaxation processes. $D = 2, r = 0.1$ (—), **and** $r = 0.0001$ (- -).

AS-93-263

Steady shock profiles are shown in Fig. 2.12 for $D = 2$ (weak nonlinear effects) and two different bandwidths of the relaxation distribution, $r = 0.1$ and $r = 0.0001$.*

*For these two cases, although the values of μ (0.278 and 0.250, respectively) are not very small, Eq. 2.20 is still dominated by the first term. Difficulties were encountered for values of $\mu = 0.5$ or larger.

A slight asymmetry can be seen, similar to that which occurs when relaxation is due to just a single process.[26] Although solutions for stronger waves have not yet been obtained, behavior similar to that for single-process relaxation is to be anticipated; that is, the asymmetry should grow as D decreases. In the single relaxation case the waveform becomes multivalued for values $D < D_{\min}$;[26] in this regime relaxation is not strong enough to prevent nonlinear steepening from causing the wave to fold over on itself. Whether distributing the relaxation process over a wide frequency band strengthens the opposition to steepening, so that multivaluedness is either delayed or perhaps even prevented, is not yet known (but see the results in the next subsection). It can be seen from the form of Eq. 2.20, however, that since the rise time of the shock is proportional to $1/\mu$, and thus to D, the shock is expected to become thinner as D decreases.

Figure 2.12 shows the shock profile to be relatively insensitive to the value of the bandwidth parameter r. The reason is that the wave shown is quite weak ($D = 2$). Most of the spectral components of the wave undoubtedly lie in the frequency region well below Ω_1. Opposition to steepening is therefore provided mainly by the lower end of the distribution band. In this case, the bandwidth of the distribution is practically irrelevant.

2.4.4 Numerical Solutions

To study the propagation of a wave that is sinusoidal at its source, Li has been developing numerical solutions of Eq. 2.18. The methods being employed are (1) spectral analysis, and (2) finite difference in the time domain. In the spectral analysis method, use of the discrete Fourier transform converts Eq. 2.18 to a system of coupled, ordinary, nonlinear, differential equations for the harmonic components. The system of equations can easily be solved numerically, for example, by a Runge Kutta algorithm. Spectral analysis works well when the wave is weak. When the wave is strong, however, a very large number of harmonic components must be retained if the shocks are to be described faithfully; consequently the computation time is long. The finite difference method should be suitable in this case, and work on it is in progress.

Figure 2.13 shows waveforms obtained by the spectral analysis method. Each set of four curves shows the progressive distortion and decay of the wave as σ increases from 0 to 5. The first two sets are for a (a) weak wave and (b) a stronger wave. Comparison shows that, as expected, the stronger wave has shorter shock rise time and more asymmetry of waveform. The ringing on the $\sigma = 3$ curve in (b) is Gibbs' phenomenon and illustrates the difficulty encountered with the spectral analysis method when the wave is strong. Notice that at $\sigma = 5$ the ringing has practically disappeared. At this distance relaxation has gained the upper hand in its battle with nonlinear steepening, and the shock has dispersed to the point that the number of

harmonic components retained (in this case 100) is enough to give a true picture of the waveform. The wave shown in (c) has the same strength as the one in (b), but the bandwidth of the relaxation processes is an order of magnitude greater. The nearly complete absence of ringing for the profiles in (c) implies that wider bandwidth does strengthen the absorption capability of the medium.

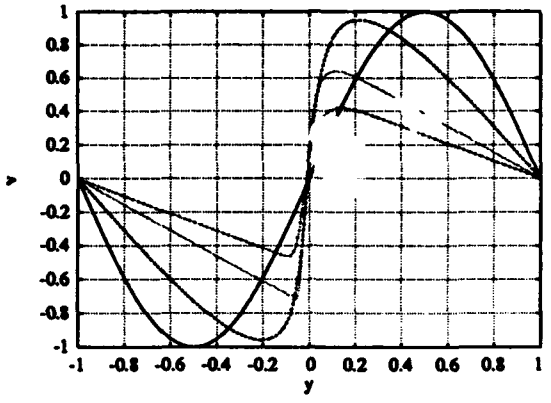

(a)
D=0.5, r=0.1

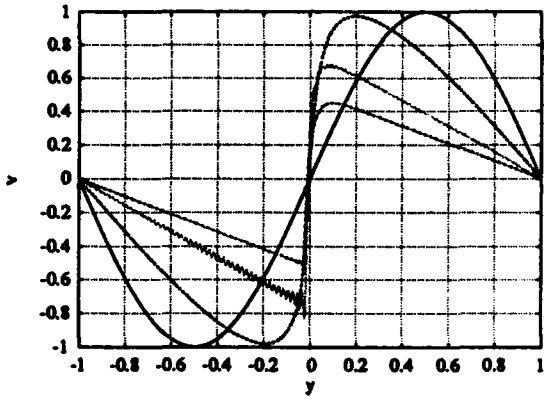

(b)
D=0.25, r=0.1

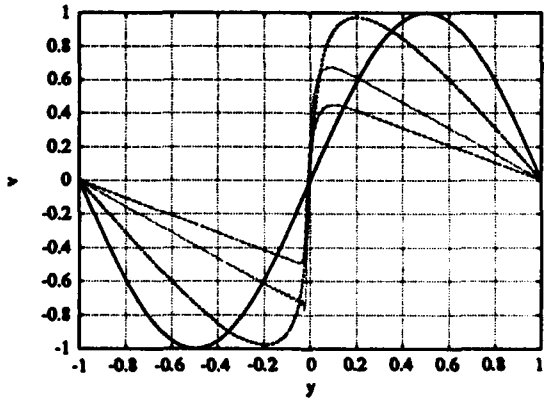

(c)
D=0.25, r=0.01

FIGURE 2.13
Waveform distortion for an originally sinusoidal wave at various distances from the source: $(—)\sigma = 0, (- \ -)\sigma = 1, (\cdots)\sigma = 3, (\cdot \ - \ \cdot \ -)\sigma = 5.$

AS-93-264

2.5 Production of an Isolated Negative-Pressure Pulse in Water

This project was motivated by a desire to produce an isolated negative-pressure pulse in water. It was felt that such a pulse would be useful in medical ultrasonics and cavitation research. Preliminary experiments by D. T. Blackstock and E. L. Carstensen at the University of Rochester in summer 1991 showed that an underwater spark, a circular aperture, and an irregularly shaped disk can be used to produce an isolated negative pulse. In September 1991 Bailey began the more careful and systematic set of experiments that are described here.

Our approach is based on the fact that diffraction by a circular aperture causes phase reversal of any incident wave. In our experiment the incident wave is the positive pulse radiated by an underwater spark. Forward scattering by a circular aperture then yields an on-axis signal that consists of a positive pulse (the incident, or direct, wave) followed by its time-delayed, inverted replica (the scattered, or edge, wave). If an irregular disk is then placed in the aperture to block the direct wave, the axial signal is just the edge wave, a negative pulse. Although the blocking disk does produce scattering, the scattering is incoherent because of the irregularity of the disk edge. Compared to the edge wave from the aperture (on axis), therefore, the disk-scattered signal is negligible.

Bailey's project has had three parts this year:

(1) Design and construct an underwater spark source, and measure the acoustic radiation.

(2) Carry out the experiment to achieve an isolated negative-pressure pulse.

(3) Investigate the "obliquity factor" that arises when the Helmholtz-Kirchhoff integral theorem is used to predict diffraction.

The first two parts have been completed, and some work has been done on the third. In addition, success with part 2 led to several related experiments that have much promise.

A general sketch of the experiment is shown in Fig. 2.14. The acoustical action takes place in a 29 × 57 cm plexiglass tank filled to a depth of 25 cm with deionized water. The underwater spark source is the open end of an RG-58 coaxial cable. The spark itself is an arc of current from the center anode to the braided annular ground of the cable. The rather complicated circuit that releases the current is described as follows. A Glassman EH20P high voltage power supply applies 8 kV to charge a 0.1 μF capacitor, which is in parallel with the series combination of the coaxial-cable

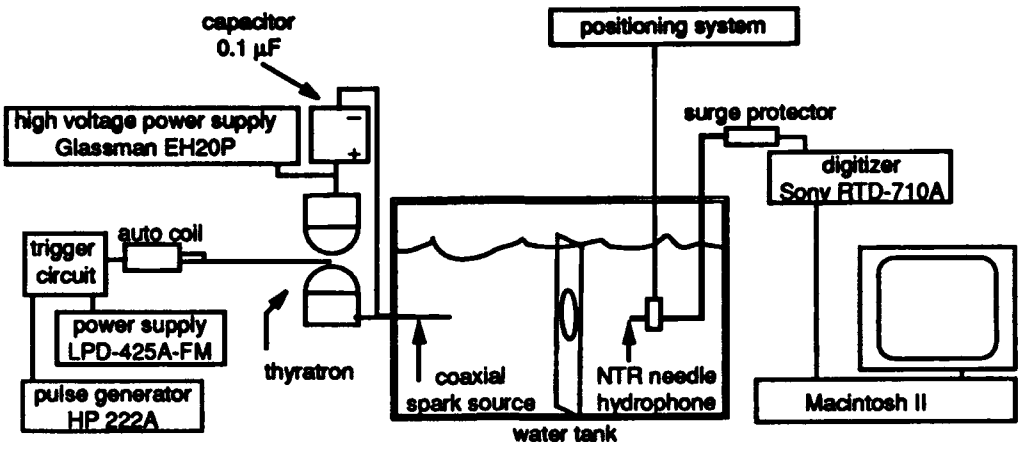

FIGURE 2.14
Spark source and experimental setup. AS-93-265

spark source and a switch. The switch is an open air thyratron, which consists of two primary electrodes and a third (ignition) electrode located in the air gap between the primary electrodes. Closure of the switch begins when a trigger circuit and GM 043 automobile coil effectively amplify a (manually initiated) voltage pulse from a Hewlett Packard 222A pulse generator. Application of the amplified potential to the ignition electrode stimulates breakdown between the primary electrodes of the thyratron switch. With the switch closed, the capacitor is free to discharge across the exposed tip of the RG-58 coaxial cable. To hold the tip fixed, Bailey mounted the end of the cable in a lucite plate (not shown in Fig. 2.14).

The spark produces a sharp positive pressure spike which, a few centimeters away, has an amplitude of about 1 MPa and a duration of about 1 μs. Since the waveform of a spherical wave cannot be truly unipolar, it is assumed that the positive spike is followed by a long, shallow negative tail, which is masked in the actual measurement by noise that follows the arrival of the pulse.

The acoustical measuring system begins with an NTR piezoceramic TNU100A needle hydrophone. The electrical output goes to a Sony-Tektronix RTD-710A (real-time digitizer), which records the measurement. LabVIEW and Matlab programs run on a Macintosh II computer are used to analyze the data. In series between the hydrophone and the digitizer, Alpha Delta Transi-trap surge protectors and 3.3 V Zener diodes protect the digitizer and reduce the electromagnetic pulse (EMP) produced by the spark. A great deal of time and energy was spent in finding a system and arrangement to prevent the EMP from interfering with the acoustical measurement. No preamplifier is presently utilized, though one is needed when Bailey uses a NTR PVDF NP-1000 needle hydrophone.

The circular aperture, on which the positive pulse is incident, is a hole in a flat baffle. The baffle itself should not transmit sound. We use an aluminum plate,

thickness 2.29 mm, covered on the incident wave side with a 1.59 mm (1/16 in.) thick sheet of corprene. The corprene is called a mask in Fig. 2.15. The aluminum, which

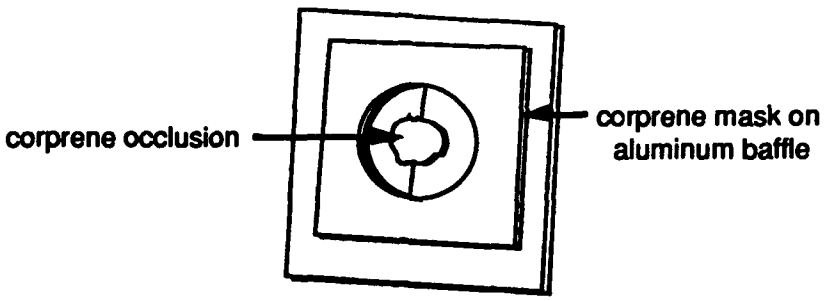

FIGURE 2.15
Occlusion and baffle construction. AS-93-266

contributes little transmission loss on its own, functions primarily as a rigid surface on which to mount the corprene, which is too flexible to use by itself. Corprene, a gasket material made of cork and neoprene, is well known for its very high acoustical transmission loss. Corprene is sometimes described as a pressure release material (it does contain air pockets) and sometimes as a very lossy material. Regardless of its actual properties, however, it does prevent sound from passing through to the back side of the baffle. The aperture is a 50 mm diam hole cut in the corprene. The companion hole in the aluminum is 1 mm larger in diameter in order that the edge presented to the incident wave be corprene, not alumimum. Moreover, to keep the apparent thickness of the baffle as small as possible, Bailey beveled the hole cut in the aluminum (sharp edge next to the corprene). The irregular disk, or occlusion, used to block the direct wave is also made of 1.59 mm thick corprene and has a diameter that varies irregularly from about 3 mm to about 4 mm. Since a slight curl of the corprene surface simply adds to the incoherence of the scattered wave, it was not necessary to back the occlusion with aluminum. The occlusion was suspended in the aperture with thread; a "crosshairs" arrangement was used (see Fig. 2.15).

Some preliminary results are shown in Fig. 2.16 for a case in which the spark-aperture distance was 8 cm and the aperture-receiver distance about 6 cm. On the left is the axial signal received when the aperture was not occluded. The initial pulse is the direct wave from the spark, a positive spike followed by some low amplitude noise that may be due to reverberation around or vibration of the tip of the RG-58 cable. Arriving about 6 μs after the direct wave is the edge wave (the 6μs delay is appropriate for the distances used in this particular experiment). As expected, the edge wave is a phase-inverted replica of the direct wave. After the corprene occlusion was inserted in the aperture, the signal became that shown in the right-hand picture. The edge wave is unchanged, but the direct wave is practically gone. Where the direct wave used to be is only a little noise, which may represent the incoherent contribution from the irregular edge of the occlusion. Notice that the noise begins about 1.5 μs

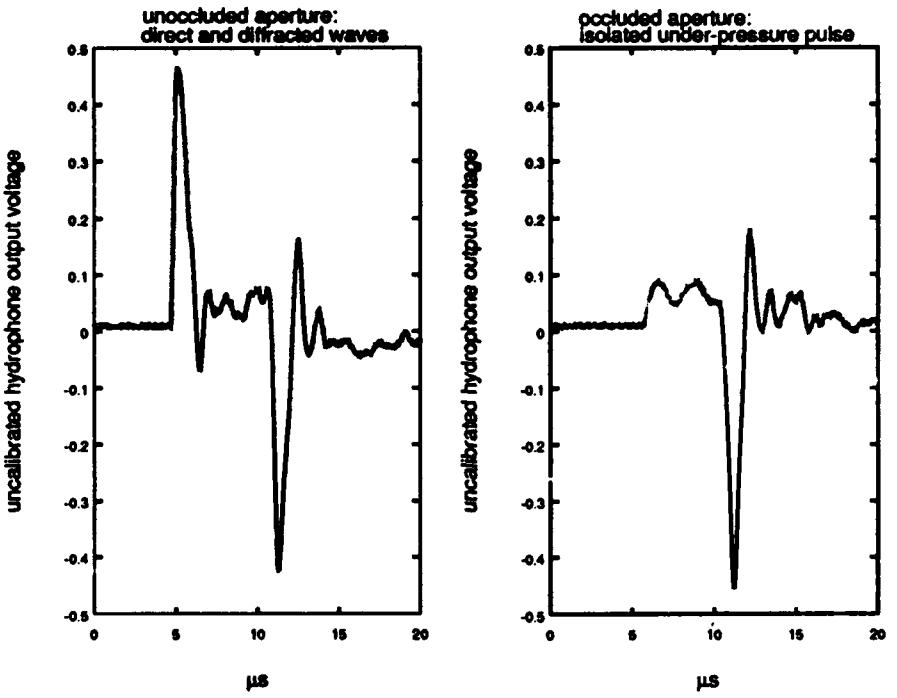

FIGURE 2.16
Data comparison: unoccluded and occluded aperture.

AS-93-267

later than the onset of the direct wave in the left-hand picture. This delay is about what one would expect for a signal scattered from the nearest edge of the occlusion.

Figure 2.16 demonstrates that the apparatus does produce the desired isolated negative-pressure pulse. Moreover, the negative pulse exists only locally. It is not spread over a wide area as it would be if generated by reflection from the water-air interface. The localized nature of the negative pulse produced by diffraction may be very advantageous in applications.

The third phase is currently under study, but measurements so far are inconclusive. Also being investigated are some other phenomena associated with irregular-edge diffraction. For example, barriers used along roadways to reduce traffic noise might be more effective if the top of the barrier were irregular rather than straight. An irregular edge would reduce the coherence of the diffracted wave that penetrates into the shadow zone behind the barrier.

The results of this project are scheduled to be presented at the New Orleans Meeting of the Acoustical Society of America, 31 October - 4 November 1992.[27]

2.6 Miscellaneous

A paper was given at the Fall 1991 Meeting of the Acoustical Society of America to report results obtained by Wright and Blackstock on the ellipsoidal focusing project (91-6).

Last year's report[1] (91-5, Section 2.4) contains a draft of a letter to the editor prepared by F. D. Cotaras and C. L. Morfey on properties of sea water and fresh water for calculations involving finite-amplitude sound. The letter has been submitted to the Journal of the Acoustical Society of America for publication (92-1).

Bradley attended the Physical Acoustics Summer School, which was sponsored by ONR and the Acoustical Society of America, in Asilomar, California, 24 June - 1 July 1992.

3. SUMMARY

Research during the current report period, 1 October 1991 – 30 September 1992, has been done on the following projects.

1. Propagation in a periodic waveguide
2. Scattering of sound by sound
3. Finite-amplitude waves in a three-layer fluid
4. Finite-amplitude waves in a medium having a distribution of relaxation processes
5. Propagation of an isolated negative-pressure pulse in water

Four topics under Project 1 were explored: (1) anisotropic periodic waveguides, (2) asymptotic behavior of small-signal Bloch wave pulses, (3) nonlinear behavior of Bloch wave pulses, and (4) group velocity of Bloch wave pulses in the stop band. The work on Project 2 was completed, except for the conversion of Ten Cate's dissertation to a technical report and the publication of two journal articles that are planned. After a high precision positioning system, which will be very useful in a variety of acoustical experiments, had been completed under Project 3, work was begun on an experiment to measure backward reradiation of second-harmonic sound from a steel plate in water. A generalized Burgers equation for tissue was developed under Project 4, and work was done to obtain some asymptotic and numerical solutions of the equation. In Project 5 an electrical spark, a circular aperture, and an irregular blocking disk were used to produced a unipolar negative pressure pulse in water. Finally, miscellaneous topics included ellipsoidal focusing of N waves and tabulation of certain useful quantities for making calculations of finite-amplitude sound in water.

REFERENCES

1. D. T. Blackstock, "Nonlinear Acoustics: Propagation in a Periodic Waveguide, Scattering of Sound by Sound, Propagation through a Three-Layer Fluid, and Nonlinearity Parameters of Sea Water," Third Annual Summary Report under Grant N00014-89-J-1109, Technical Report ARL-TR-91-21, Applied Research Laboratories, The University of Texas at Austin, 19 August 1991 (AD A241 294).

2. J. D. Jackson, *Classical Electrodynamics* (John Wiley and Sons, Inc., New York, 2nd ed., 1975).

3. D. T. Blackstock, "Nonlinear Acoustics: Propagation in a Periodic Waveguide and Scattering of Sound by Sound" Second Annual Summary Report under Grant N00014-89-J-1109, Technical Report ARL-TR-90-21, Applied Research Laboratories, The University of Texas at Austin, 17 July 1990 (AD A224 738).

4. Jarle Berntsen, Jacqueline Naze Tjøtta, and Sigve Tjøtta, "Nearfield of a large acoustic transducer. Part IV: Second harmonic and sum frequency radiation," *J. Acoust. Soc. Am.* **75**, 1383–1391 (1984).

5. J. Naze Tjøtta and S. Tjøtta, "Interaction of sound waves, Part I: Basic equations and plane waves," *J. Acoust. Soc. Am.* **82**, 1425–1428 (1987).

6. J. Naze Tjøtta and S. Tjøtta, "Interaction of sound waves, Part II: Plane waves and real beam," *J. Acoust. Soc. Am.* **82**, 1429–1435 (1987).

7. J. Naze Tjøtta and S. Tjøtta, "Interaction of sound waves, Part III: Two real beams," *J. Acoust. Soc. Am.* **83**, 487–495 (1988).

8. J. Berntsen, J. Naze Tjøtta, and S. Tjøtta, "Interaction of sound waves. Part IV: Scattering of sound by sound," *J. Acoust. Soc. Am.* **86**, 1968–1983 (1989).

9. S. I. Aanonsen, T. Barkve, J. Naze Tjøtta, and S. Tjøtta, "Distortion and harmonic generation in the nearfield of a finite amplitude sound beam," *J. Acoust. Soc. Am.* **75**, 749–768 (1984).

10. M. F. Hamilton, J. Naze Tjøtta, and S. Tjøtta, "Nonlinear effects in the farfield of a directive sound source," *J. Acoust. Soc. Am.* **78**, 202–214 (1985).

11. J. Naze Tjøtta, S. Tjøtta, and E. Vefring, "Propagation and interaction of two collinear finite amplitude sound beams," *J. Acoust. Soc. Am.* **88**, 2859–2870 (1990).

12. J. Berntsen, "Numerical calculations of finite amplitude sound beams," in *Frontiers of Nonlinear Acoustics – 12th ISNA*, M. F. Hamilton and D. T. Blackstock, eds. (Elsevier Applied Science, London, 1990), pp. 191–196.

13. J. Berntsen, T. O. Epselid, and A. Genz, "An automatic integration routine applicable in linear and nonlinear acoustics," in *Frontiers of Nonlinear Acoustics – 12th ISNA*, M. F. Hamilton and D. T. Blackstock, eds. (Elsevier Applied Science, London, 1990), pp. 609–614.

14. R. K. Gould, C. W. Smith, A. O. Williams, Jr., and R. P. Ryan, "Measured structure of harmonics self-generated in an acoustic beam," *J. Acoust. Soc. Am.* **40**, 421–427 (1966).

15. C. M. Darvennes and M. F. Hamilton, "Scattering of sound by sound from two Gaussian beams," *J. Acoust. Soc. Am.* **87**, 1955–1964 (1990).

16. V. E. Nazarov, "Frequency doubling of an acoustic wave on a nonlinear layer," *Soviet Phys. Acoust.* **36**, 398-399 (1990).

17. R. T. Beyer, *Nonlinear Acoustics*, (Dept. of Navy, 1974), Ch. 3.

18. E. L. Carstensen, N. D. McKay, D. Dalecki, and T. G. Muir, "Absorption of finite amplitude ultrasound in tissues," *Acustica* **51**, 116-123 (1982).

19. D. T. Blackstock, "On the absorption of finite-amplitude sound," *Frontiers of Nonlinear Acoustics – 12th ISNA*, ed. M. F. Hamilton and D. T. Blackstock, eds. (Elsevier Applied Science, London, 1990), pp. 119-124.

20. D. T. Blackstock, "Thermoviscous attenuation of plane, periodic, finite-amplitude waves," *J. Acoust. Soc. Am.* **36**, 534-542 (1964).

21. D. T. Blackstock, "Generalized Burgers equation for plane waves," *J. Acoust. Soc. Am.* **77**, 2050-2053 (1985).

22. E. L. Carstensen and H. P. Schwan, "Acoustic properties of hemoglobin solutions," *J. Acoust. Soc. Am.* **31**, 305-311 (1959).

23. D. Dalecki, E. L. Carstensen, K. J. Parker, and D. R. Bacon, "Absorption of finite amplitude focused ultrasound," *J. Acoust. Soc. Am.* **89**, 2435–2447 (1991) and "Erratum," *J. Acoust. Soc. Am.* **90**, 2855 (1991).

24. H. A. Jongen, J. M. Thijssen, M. Van der Aarssen, and W. A. Verhock, "A general model for the absorption of ultrasound by biological tissues and experimental verification," *J. Acoust. Soc. Am.* **79**, 535-540 (1986).

25. S. I. Soluyan and R. V. Khokhlov, "Finite amplitude acoustic waves in a relaxating medium," *Soviet Phys. Acoust.* **8**, 170-175 (1962).

26. O. V. Rudenko and S. I. Soluyan, *Theoretical foundations of nonlinear acoustics*, Ch. 4, (Consultants Bureau, 1977).

27. M. R. Bailey, D. T. Blackstock, and E. L. Carstensen, "Isolation of a negative pressure pulse by means of diffraction," Paper 3aPA6, 124th Meeting, Acoustical Society of America, New Orleans, Louisiana, 31 October - 4 November 1992. ABSTRACT: *J. Acoust. Soc. Am.* **94**, 2359 (1992).

CHRONOLOGICAL BIBLIOGRAPHY
1988-1992

CHRONOLOGICAL BIBLIOGRAPHY
1988–1992
Grant N00014-89-J-1109
and
Predecessor Contract N00014-84-K-0574 (ended 9-30-88)

Code			ONR Grant/Contract		
B	=	chapter in a book	1109	=	N00014-89-J-1109, began 10-1-88
J	=	journal publication			
JS	=	submitted for journal publication	0574	=	N00014-84-K-0574, ended 12-31-88
O	=	oral presentation			
P	=	paper in a proceedings			
T	=	thesis or dissertation	0867	=	N00014-75-C-0867 ended 8-31-84
TR	=	technical report			

1988

ONR Contract	Code		
0574	J	[a]1.	M. F. Hamilton and D. T. Blackstock, "On the coefficient of nonlinearity β in nonlinear acoustics," *J. Acoust. Soc. Am.* **83**, 74–77 (1988).
0574	O	[b,c]2.	D. T. Blackstock, "Shock wave propagation and shape of the waveform," Conference on Lithotripsy (Extra-Corporeal Shock Wave Applications - Technical and Clinical Problems), University of Florida, Gainesville, 12–13 March 1988.
0574	O	[b]3.	D. T. Blackstock, "Calculation of the intensity and absorption of a finite-amplitude sound wave," Paper B8, 115th Meeting, Acoustical Society of America, Seattle, 16-20 May 1988. ABSTRACT: *J. Acoust. Soc. Am.* **83**, S5 (1988).
0574	O	[b]4.	D. T. Blackstock, "Physical aspects of lithotripsy," Paper GG1, 115th Meeting, Acoustical Society of America, Seattle, 16-20 May 1988. ABSTRACT: *J. Acoust. Soc. Am.* **83**, S71 (1988).

[a]Hamilton's support for this work came from Contract N00014-85-K-0708.

[b]Primary support for this work came from University of Rochester, NIH Grant CA 39241.

[c]Partial support for this work came from a grant from Bureau of Engineering Research, College of Engineering, The University of Texas at Austin.

ONR Contract	Code		
0574	TR	5.	D. T. Blackstock, "Nonlinear Acoustics: Reflection and Refraction, Scattering of Sound by Sound, and Periodic Media," Fourth Annual Summary Report under Contract N00014-84-K-0574, Technical Report ARL-TR-88-30, Applied Research Laboratories, The University of Texas at Austin, 30 June 1988 (AD A197 614).
0867	J	6.	M. F. Hamilton and J. A. Ten Cate, "Finite amplitude sound near cutoff in higher order modes of a rectangular duct," *J. Acoust. Soc. Am.* **84**, 327-334 (1988).
Gen§	O	7.	D. T. Blackstock, I. J. Busch-Vishniac, M. F. Hamilton, and E. L. Hixson, "Graduate acoustics at The University of Texas at Austin," Paper ZZ9, 116th Meeting, Acoustical Society of America, Honolulu, 14-18 November 1988. ABSTRACT: *J. Acoust. Am.* **84**, S167 (1988).

§Although no specific grant or contract can be cited, it is appropriate to acknowledge ONR because its support of research in physical acoustics at U. T. Austin has played an important role in the development of the University's graduate acoustics program.

ONR Contract	Code		
1109 0574	T,TR	1.	F. D. Cotaras, "Reflection and Refraction of Finite Amplitude Acoustic Waves at a Fluid-Fluid Interface," Ph.D. dissertation, Electrical and Computer Engineering Department, The University of Texas at Austin, May 1989. Also issued as Technical Report ARL-TR-89-1, Applied Research Laboratories, The University of Texas at Austin (3 January 1989). (AD A209800) ABSTRACT: *J. Acoust. Soc. Am.* **92**, S201 (1991).
1109	O	[d]2.	D. T. Blackstock, S. Cheng, M. R. Jones, and W. M. Wright, "Focusing of intense sound pulses by an ellipsoidal reflector," Paper BE12, Joint Spring Meeting, Texas Sections of American Association of Physics Teachers and American Physical Society, University of Houston, Houston, 3–4 March 1989.
1109	O	[d]3.	S. T. W. Cheng, M. R. Jones, D. T. Blackstock, and W. M. Wright, "Focusing of an N wave by an ellipsoidal reflector: An experiment in air," Paper TT12, 117th Meeting, Acoustical Society of America, Syracuse, 22–26 May 1989. ABSTRACT: *J. Acoust. Soc. Am.* **85**, S113 (1989).
1109 0574	O	4.	C. E. Bradley, "Finite amplitude acoustic propagation in a periodic structure," Paper B12, 117th Meeting, Acoustical Society of America, Syracuse, 22–26 May 1989. ABSTRACT: *J. Acoust. Soc. Am.* **85**, S6 (1989).
1109 0574 0867	O	5.	D. T. Blackstock, "Physical aspects of nonlinear acoustics," invited review paper, Conference for Ultrasonics in Biophysics and Bioengineering, Allerton Park, Monticello, Illinois, 30 May–2 June 1989.
1109	TR	6.	D. T. Blackstock, "Nonlinear Acoustics: Reflection and Refraction, Propagation in a Periodic Waveguide, Scattering of Sound by Sound, and Ellipsoidal Focusing," First Annual Summary Report under Grant N00014-89-J-1109, Technical Report ARL-TR-89-38, Applied Research Laboratories, The University of Texas at Austin, 31 July 1989. (AD A211412)

[d]Primary support for this work came from Applied Research Laboratories IR&D program and Texas Advanced Research Program.

ONR Contract	Code		
1109 0574	O,P	7.	F. D. Cotaras, D. T. Blackstock, S. Tjøtta, and J. Naze Tjøtta, "An analysis of the reflection and refraction of finite-amplitude plane waves at a plane fluid-fluid interface," 13th International Congress on Acoustics, Belgrade, Yugoslavia, 24–31 August 1989. Proceedings, Vol. I, pp. 263–266 (1989).
1109 0574	O,P	[e]8.	J. Naze Tjøtta, J. A. Ten Cate, and S. Tjøtta, "Scattering of sound by sound: Effects of boundary conditions," 13th International Congress on Acoustics, Belgrade, Yugoslavia, 24–31 August 1989. Proceedings, Vol. I, pp. 287–290 (1989).
1109 0574	O	[e]9.	J. Naze Tjøtta, J. A. Ten Cate, and S. Tjøtta, "Effects of boundary conditions on the propagation and interaction of finite amplitude sound beams," Paper PP2, 118th Meeting, Acoustical Society of America, St. Louis, 27 November–1 December 1989. ABSTRACT: *J. Acoust. Soc. Am.* **86**, S106 (1989).

[e]Partial support for this work came from Applied Research Laboratories IR&D program.

ONR Contract	Code		
Gen[§]	O	1.	D. T. Blackstock, "Evanescent waves in acoustics," Paper AC1, Joint Spring Meeting, Texas Sections of American Association of Physics Teachers and American Physical Society, Texas Christian University, Fort Worth, Texas, 2–3 March 1990. ABSTRACT: *Bull. Am. Phys. Soc.* **35**, 1328 (1990).
1109 0574 0867	O	[f]2.	D. T. Blackstock and J. D. Maynard, "Demonstration of nonlinear acoustics phenomena," Paper L6, 119th Meeting, Acoustical Society of America, Pennsylvania State University, 21–25 May 1990. ABSTRACT: *J. Acoust. Soc. Am.* **87**, S32 (1990).
1109	O	3.	C. E. Bradley, "Linear and nonlinear acoustic propagation in a periodic waveguide," Paper TT9, 119th Meeting, Acoustical Society of America, Pennsylvania State University, 21–25 May 1990. ABSTRACT: *J. Acoust. Soc. Am.* **87**, S113 (1990).
1109	TR	4.	D. T. Blackstock, "Nonlinear Acoustics: Propagation in a Periodic Waveguide and Scattering of Sound by Sound," Second Annual Summary Report under Grant N00014-89-J-1109, Technical Report ARL-TR-90-21, Applied Research Laboratories, The University of Texas at Austin, 17 July 1990. (AD A224 738)
1109 0574	O,P	[g]5.	D. T. Blackstock, "On the absorption of finite-amplitude sound," 12th International Symposium on Nonlinear Acoustics, Austin, Texas, 27–31 August 1990, in *Frontiers of Nonlinear Acoustics – 12th ISNA*, M. F. Hamilton and D. T. Blackstock, eds. (Elsevier Applied Science, London, 1990), 119–124.

[f]Maynard's support for this work came from an ONR contract at Pennsylvania State University.

[g]Partial support for this work came from NIH Grant CA 49172 and from University of Rochester NIH Grant CA 39241.

ONR Contract	Code		
0574 0867	O,P	[h]6.	D. A. Nelson and D. T. Blackstock, "Harmonic generation, propagation and attenuation for finite-amplitude tones in an air-filled porous material," 12th International Symposium on Nonlinear Acoustics, Austin, Texas, 27–31 August 1990, *Frontiers of Nonlinear Acoustics – 12th ISNA*, M. F. Hamilton and D. T. Blackstock, eds. (Elsevier Applied Science, London, 1990) 621–626.
1109 0574	O,P	7.	C. E. Bradley, "Linear and nonlinear acoustic propagation in a periodic waveguide," 12th International Symposium on Nonlinear Acoustics, Austin, Texas, 27–31 August 1990, in *Frontiers of Nonlinear Acoustics – 12th ISNA*, M. F. Hamilton and D. T. Blackstock, eds. (Elsevier Applied Science, London, 1990) 315–320.
1109	Book	[i,j]8.	M. F. Hamilton and D. T. Blackstock, eds., ***Frontiers of Nonlinear Acoustics – 12th ISNA*** (Elsevier Applied Science, London, 1990).
1109	J	[i]9.	M. F. Hamilton and D. T. Blackstock, "On the linearity of the momentum equation for progressive plane waves of finite amplitude," *J. Acoust. Soc. Am.* **88**, 2025–2026 (1990).
1109	O	10.	D. T. Blackstock, "Nonlinear Acoustics," Rayleigh Lecture, Winter Annual Meeting, American Society of Mechanical Engineers, Dallas, Texas, 25–30 November 1990.
1109	T	11.	C. E. Bradley, "Acoustic Bloch Wave Propagation in a Periodic Waveguide," M.S. thesis, Mechanical Engineering Department, The University of Texas at Austin, December 1990.

[h]Primary support for this work came from NASA Grant NSG 3198.

[i]Hamilton's support for this work came from Grant N00014-89-J-1003.

[j]Also supported in part by Grant N00014-J-90-1373.

C.R Contract	Code		
1109 0574	J	[e]1.	J. Naze Tjøtta, J. A. Ten Cate, and S. Tjøtta, "Effects of boundary conditions on the nonlinear interaction of sound beams," *J. Acoust. Soc. Am.* **89**, 1037–1049 (1991).
1109	O	2.	Charles E. Bradley and David T. Blackstock, "Acoustic Bloch wave energy transport and group velocity," Paper 7PA4, 121st Meeting, Acoustical Society of America, Baltimore, Maryland, 29 April – 3 May 1991. ABSTRACT: *J. Acoust. Soc. Am.* **89**, 1971 (1991).
1109	O	[k]3.	David T. Blackstock and Christopher L. Morfey, "Reflection and transmission of spherical waves incident on a concentric spherical interface," Paper 7PA1, 121st Meeting, Acoustical Society of America, Baltimore, Maryland, 29 April – 3 May 1991. ABSTRACT: *J. Acoust. Soc. Am.* **89**, 1971 (1991).
1109	TR	4.	C. E. Bradley, "Acoustic Bloch Wave Propagation in a Periodic Waveguide," Technical Report ARL-TR-91-19, Applied Research Laboratories, The University of Texas at Austin, 24 July 1991. (AD A244-068)
1109	TR	5.	D. T. Blackstock, "Nonlinear Acoustics: Propagation in a Periodic Waveguide, Scattering of Sound by Sound, Propagation Through a Three-Layer Fluid, and Nonlinearity Parameters of Sea Water," Third Annual Summary Report under Grant N00014-89-J-1109, Technical Report ARL-TR-91-21, Applied Research Laboratories, The University of Texas at Austin, 19 August 1991. (AD A241 294)
1109	O	6.	W. M. Wright and D. T. Blackstock, "Experimental study of ellipsoiodal focusing of spark-produced N waves in air," *J. Acoust. Soc. Am.* **90**, 2339(A) (1991), Paper 7PA6 (invited) 122nd Meeting, Acoustical Society of America, Houston, Texas, 4 – 8 November 1991.
1109	O	7.	James A. Ten Cate, "Measurements of nonlinear effects in the sound field radiated from a circular piston in water," Paper 2PA2, *J. Acoust. Soc. Am.* **90**, 2244(A) (1991).

[k]Also supported in part by Grant NAG-1-1204 and University of Southampton, England.

ONR Contract	Code		
1109	JS	1.	F. D. Cotaras and C. L. Morfey, "Polynomial expressions for the coefficient of nonlinearity β and $\beta(\rho c^5)^{1/2}$ for fresh water and sea water," submitted April 1992 for publication in *J. Acoust. Soc. Am.*
1109	O	2.	James A. Ten Cate, "Scattering of Sound by Sound: Nonlinear Interaction of Collinear and Noncollinear Sound Beams," Ph.D. dissertation, Mechanical Engineering Department, The University of Texas at Austin, May 1992.
1109	O	3.	D. T. Blackstock, "Stories about F. V. Hunt's Acoustics Research Laboratory (Harvard) and about nonlinear acoustics," paper 3pED2, 124th Meeting, Acoustical Society of America, New Orleans, Louisiana, 31 October – 4 November 1992. ABSTRACT: *J. Acoust. Soc. Am.* **94**, 2378 (1992).
1109	O	4.	M. R. Bailey, D. T. Blackstock, and E. L. Carstensen, "Isolation of a negative pressure pulse by means of diffraction," Paper 3aPA6, 124th Meeting, Acoustical Society of America, New Orleans, Louisiana, 31 October – 4 November 1992. ABSTRACT: *J. Acoust. Soc. Am.* **94**, 2359 (1992).

DISTRIBUTION LIST FOR
ARL-TR-93-11
UNDER GRANT N00014-89-J-1109
FOURTH ANNUAL SUMMARY REPORT

Copy No.	
	Director Advanced Research Projects Agency 3701 North Fairfax Dr. Arlington, VA 22203-1714
1	Attn: Technical Library
	Office of Naval Research Physics Division Office (Code 3120) 800 North Quincy Street
2-3	Arlington, VA 22217-5660
	Office of Naval Research 800 North Quincy Street Arlington, VA 22217-5000
4	Attn: Code 20
	Naval Research Laboratory Department of the Navy (Code 2625) Washington, DC 20375-5000
5	Attn: Technical Library
	Office of the Director of Defense Research and Engineering Information Office Library Branch The Pentagon, Rm. 3E 1006
6	Washington, DC 20301
	U.S. Army Research Office Box 12211 Research Triangle Park
7-8	North Carolina 27709-2211
	Defense Technical Information Center Cameron Station, Building 5
9-10	Alexandria, VA 22314
	Director, National Bureau of Standards Research Information Center Gaithersburg, MD 20899
11	Attn: Technical Library (Admin E-01)
	Commander U.S. Army Belvior Research, Development and Engineering Ctr. Fort Belvior, VA 22060-5606
12	Attn: Technical Library (STRBE-BT)
	ODDR&E Advisor Group on Electron Devices 201 Varick Street, 11th Floor
13	New York, NY 10014-4877

Copy No.	
	Air Force Office of Scientific Research Department of the Air Force
14	Bolling AFB, DC 22209
	Air Force Weapons Laboratory Kirtland Air Force Base Albuquerque, NM 87117
15	Attn: Technical Library
	Lawrence Livermore Laboratory The University of California P.O. Box 808 Livermore, CA 94550
16	Attn: Dr. W. F. Krupke
	Naval Air Weapons Station China Lake, CA 93555-6001
17	Attn: Technical Library (Code 753)
	Naval Undersea Warfare Center Division New London, CT 06320-5994
18	Attn: Technical Center
	Commandant of the Marine Corps Scientific Advisor (Code RD-1)
19	Washington, DC 20380
	Indian Head Division Naval Surface Warfare Center Indian Head, MD 20640-5000
20	Attn: Technical Library
	Naval Postgraduate School Monterey, CA 93940
21	Attn: Technical Library (Code 0212)
	Naval Air Weapons Station Point Mugu, CA 93042-5000
22	Attn: Technical Library (Code 5632.2)
	Naval Ordnance Station Crane Division Naval Surface Warfare Center Louisville, KY 40214
23	Attn: Technical Library
	Naval Research Laboratory Stennis Space Center, MS 39529-5004
24	Attn: Technical Library

Distribution List for ARL-TR-93-11 under Grant N00014-89-J-1109 (cont'd)

Copy No.

Naval Command Control and Ocean
Surveillance Center
RDT & E Division
San Diego, CA 92152
25 Attn: Technical Library

Dahlgren Division
Naval Surface Warfare Center
Silver Spring, MD 20903-5000
26 Attn: Technical Library

Carderock Division
Naval Surface Warfare Center
Bethesda, MD 20084-5000
27 Attn: Central Library (Codes L42 and L43)

Naval Air Warfare Center
Aircraft Division, Indianpolis
Indianapolis, IN 46219-2189
28 Attn: Technical Library

Harry Diamond Laboratories
2800 Powder Mill Road
Adelphi, MD 20738
29 Attn: Technical Library

Robert E. Apfel
Yale University
P.O. Box 2159
30 New Haven, CT 06520

Yves H. Berthelot
School of Mechanical Engineering
Georgia Institute of Technology
31 Atlanta, GA 30332

Franklin R. Breckenridge
National Bureau of Standards
32 Gaithersburg, MD 20899

Edwin L. Carstensen
University of Rochester
Department of Electrical Engineering
33 Rochester, NY 14627

Peter H. Ceperly
George Mason University
Electrical & Computer Engineering Dept.
4400 University Ave.
34 Fairfax, VA 22030

Copy No.

Frederick D. Cotaras
Defence Research Establishment Atlantic
P.O. Box 1012
Dartmouth, NS B2Y 3Z6
35 Canada

Lawrence A. Crum
Applied Physics Laboratory
University of Washington
1013 N.E. 40th Street
36 Seattle, WA 98105-6698

Steven L. Garrett
Department of Physics - Code 61Gx
Naval Postgraduate School
37 Monterey, CA 93943-5000

Robert E. Gree:.
Materials Science and Engineering
The Johns Hopkins University
38 Baltimore, MD 21218

Moises Levy
Department of Physics
The University of Wisconsin - Milwaukee
39 Milwaukee, WI 53201

Philip L. Marston
Department of Physics
Washington State University
40 Pullman, WA 99164-2814

Walter G. Mayer
Department of Physics
Georgetown University
41 Washington, DC 20057

Julian D. Maynard
Department of Physics
Pennsylvania State University
42 University Park, PA 16802

Bryant E. McDonald
Naval Research Laboratory
P.O. Box 8337
43 Orlando, FL 32856

Christopher L. Morfey
ISVR
The University of Southampton
Southampton S09 5NH
44 England

Distribution List for ARL-TR-93-11 under Grant N00014-89-J-1109 (cont'd)

Copy No.

Allan D. Pierce
Department of Aerospace &
Mechanical Engineering
Boston University
110 Cummington Street
45 Boston, MA 02215

Andrea Prosperetti
The Johns Hopkins University
Department of Mechanical Engineering
46 Baltimore, MD 21218

Wolfgang H. Sachse
Theoretical and Applied Mechanics
Cornell University
47 Ithaca, NY 14853-1503

Robert N. Thurston - 3X223
Bell Communications Research
Guided Wave and Optoelectronics
331 Newman Springs Road
48 Red Bank, NJ 07701

James W. Wagner
Materials Science and Engineering
The Johns Hopkins University
49 Baltimore, MD 21218

Wayne M. Wright
Department of Physics
Kalamazoo College
50 Kalamazoo, MI 49007

51 E. L. Hixson (Electrical & Computer Engineering)

52 M. F. Hamilton (Mechanical Engineering)

53 I. Busch-Vishniac (Mechanical Engineering)

54 F. M. Pestorius, Director, ARL:UT

55 Library ARL:UT

56-60 NAD Reserve